AD_____

Award Number: W81XWH-09-1-0668

TITLE: Epigenetic Regulation of microRNA Expression: Targeting the Triple-Negative Breast Cancer Phenotype

PRINCIPAL INVESTIGATOR: Bridgette M. Collins-Burow, M.D., Ph.D.

CONTRACTING ORGANIZATION: Tulane University
New Orleans, LA 70112

REPORT DATE: October 2011

TYPE OF REPORT: Final

PREPARED FOR: U.S. Army Medical Research and Materiel Command
Fort Detrick, Maryland 21702-5012

REPORT DOCUMENTATION PAGE

Form Approved
OMB No. 0704-0188

1. REPORT DATE *(DD-MM-YYYY)*	2. REPORT TYPE	3. DATES COVERED *(From - To)*
October 2011	Final	15 Sept 2009 – 14 Sept 2011

4. TITLE AND SUBTITLE

Epigenetic Regulation of MicroRNA Expression: Targeting the Triple-Negative Breast Cancer Phenotype

5a. CONTRACT NUMBER

5b. GRANT NUMBER
W81XWH-09-1-0668

5c. PROGRAM ELEMENT NUMBER

6. AUTHOR(S)

Bridgette M. Collins-Burow

5d. PROJECT NUMBER

5e. TASK NUMBER

5f. WORK UNIT NUMBER

7. PERFORMING ORGANIZATION NAME(S) AND ADDRESS(ES)

Tulane University

New Orleans, LA 70112

8. PERFORMING ORGANIZATION REPORT NUMBER

9. SPONSORING / MONITORING AGENCY NAME(S) AND ADDRESS(ES)

US Army Medical Research
And Materiel Command
Fort Detrick, Maryland
21702-5012

10. SPONSOR/MONITOR'S ACRONYM(S)

11. SPONSOR/MONITOR'S REPORT NUMBER(S)

12. DISTRIBUTION / AVAILABILITY STATEMENT

Approved for public release; distribution unlimited

13. SUPPLEMENTARY NOTES

14. ABSTRACT

The primary long-term objective of this research is to identify HDAC inhibitor (HDACi) regulated microRNAs which regulate the epithelial-to-mesenchymal transition (EMT) in triple-negative breast cancer (TNBC). Thus far we have assessed the microRNA expression profiles of two TNBC cell lines following treatment with HDACi identifying a number of up- and down-regulated microRNAs. The overall microRNA profile after HDACi treatment was indicative of a less aggressive phenotype. Treatment with HDACi also resulted in increased expression of E-cadherin as well as decreased migration of TNBC indicating a reversal of the EMT phenotype. These results, along with our ongoing research, suggest the ability of HDACi treatment to reverse the EMT phenotype, associated with metastatic and aggressive disease, of TNBC and support future evaluation of HDACi as therapeutic options for the clinical treatment of TNBC.

15. SUBJECT TERMS
HDAC inhibitor, microRNA, triple-negative breast cancer, EMT

16. SECURITY CLASSIFICATION OF:			17. LIMITATION OF ABSTRACT	18. NUMBER OF PAGES	19a. NAME OF RESPONSIBLE PERSON
a. REPORT	b. ABSTRACT	c. THIS PAGE			USAMRMC
U	U	U	UU	66	19b. TELEPHONE NUMBER *(include area code)*

Table of Contents

Introduction.....**4**

Body.....**5**

Key Research Accomplishments.....**9**

Reportable Outcomes.....**9**

Conclusions.....**9**

References.....**10**

Appendices.....**11**

INTRODUCTION

The term 'Triple Negative Breast Cancer' (TNBC) represents a heterogeneous group of diseases and clearly does not comprise a "single entity". While triple-negative cancer is not a synonym for basal-like cancer, basal-like cancers are preferentially negative for estrogen receptor (ER) and progesterone receptor (PR) and lack human epidermal growth factor receptor 2 (HER2) expression. While it is clear that all TNBC does not fall into the basal-like phenotype and vice versa, there is microarray-based gene expression analysis demonstrating a significant overlap (1). Clinical similarities also exist between triple-negative tumors and basal-like tumors including: a higher prevalence in African-American women, greater frequency in younger patients, and a more aggressive phenotype than other molecular subgroups. EMT (epithelial to mesenchymal transition) is the process by which epithelial cells convert to mesenchymal cells and is essential in embryonic development. It appears that aberrant activation of EMT later in life drives cancer progression, and is involved in highly aggressive, poorly differentiated breast cancers with increased potential for metastasis and recurrence (2). Basal-like breast carcinomas express genes associated with an EMT phenotype and is found in normal basal/myoepithelial cells of the breast, including high-molecular-weight 'basal' cytokeratins, vimentin, and N-cadherin. Interestingly invasive breast cancers with a mesenchymal (basal-like) phenotype have been described to exhibit the loss of expression of certain miRNAs (3). MicroRNA's are a class of short non-coding RNAs found in many plants and animals and often act post-transcriptionally to inhibit gene expression. It has been shown that cells that had undergone EMT in response to TGF-β demonstrated marked downregulation of miR-200 family members, while enforced expression of miR-200 was sufficient to prevent TGFβ-induced EMT (4). Epigenetic alterations including modification of histones and others proteins by acetylation and/or phosphorylation play critical roles in the control of gene regulation. Inhibitors of HDACs (HDACi) function to block the deacetylation of histones by HDACs, which in turn blocks the inhibition of gene expression including miRNA expression. Using microRNA array analysis, a rapid alteration of miRNA levels in response to HDACi in the breast cancer cell line SKBr3 has been reported (5). The work described here tests the hypothesis that HDACi-induced increases of miRNA levels regulate the epithelial-to-mesenchymal transition in TNBC. These results indicate the potential therapeutic uses of HDACi to reverse the EMT phenotype and metastatic progression of TNBC.

Task 1. HDAC analysis of miRNA profiles in triple-negative breast cancer cells.

Completed

Results have recently been published in our manuscript "The histone deacetylase inhibitor trichostatin A alters microRNA expression profiles in apoptosis-resistant breast cancer cells", *Oncology Reports* **27**: 10-16, 2012; Additional data are included in a manuscript currently in preparation titled "The pan-deacetylase inhibitor LBH589 up-regulates anti-metastatic microRNAs miR-335 and miR-203 in triple-negative breast cancer cells" to be submitted to Cancer Research.

Task 2. qPCR validation of HDAC regulated miRNAs.

Task 2a. qPCR validation of HDAC regulated miRNAs.

This task is ongoing due to the large number of HDACi-induced changes across a variety of TNBC cell lines. Results thus far indicate consistent changes in the microarray and qPCR.

miR expression validation by independent qPCR

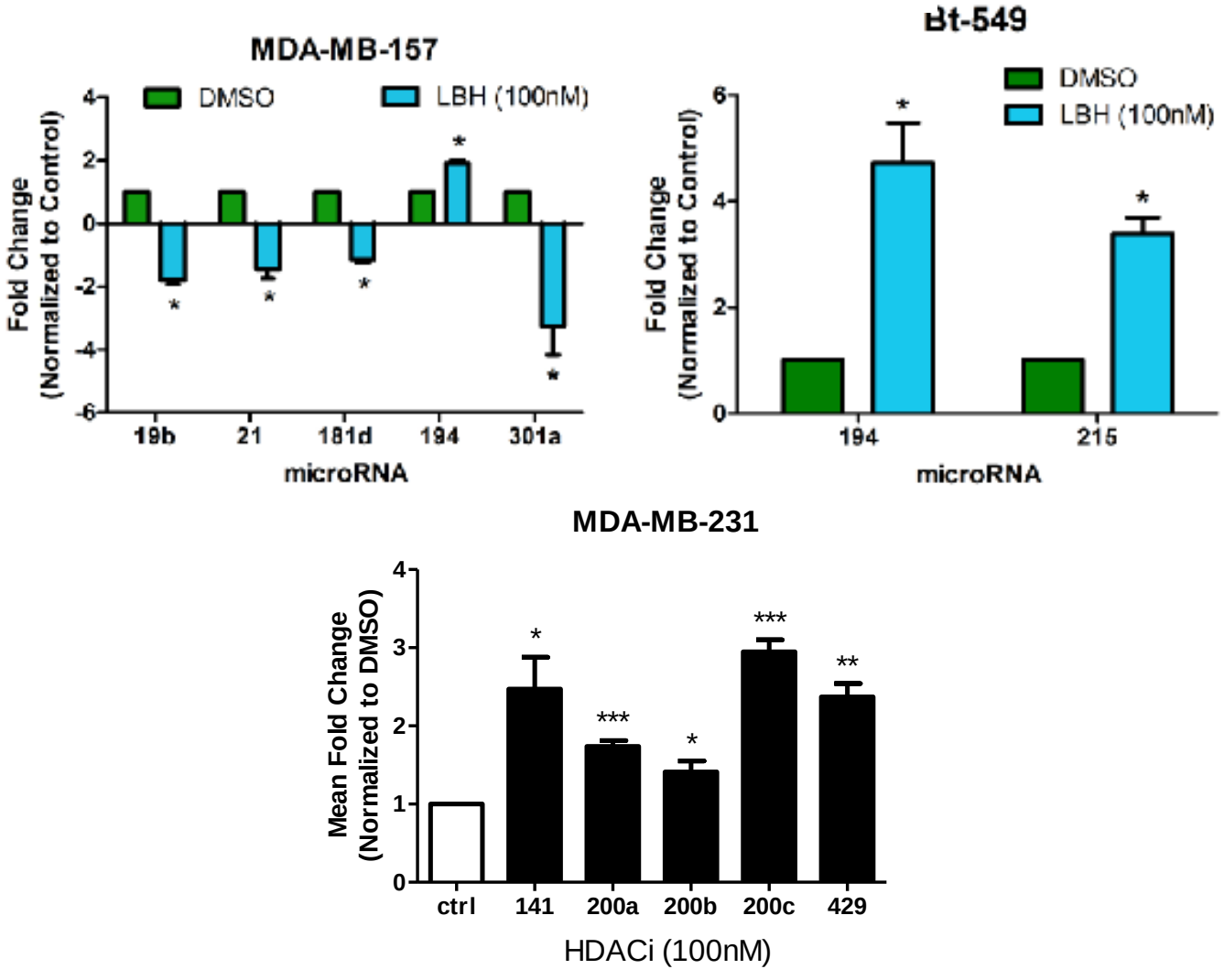

Task 2b. Determine effects of HDACi on EMT phenotype of TNBC cells.

This task is ongoing. Data in our MDA-MB-231 cells treated with HDACi (100nM) demonstrating a significant increase in E-cadherin expression by flow cytometry and ELISA, as well as increased E-cadherin protein expression by IF in xenograft tumors have been published ("Targeting triple-negative breast cancer cells with the HDAC inhibitor Panobinostat" BCR, accepted for publication April 16th, 2012). Studies examining vimentin expression, a mesenchymal cell marker, following HDACi treatment are also being conducted, but we do not have the results at this time.

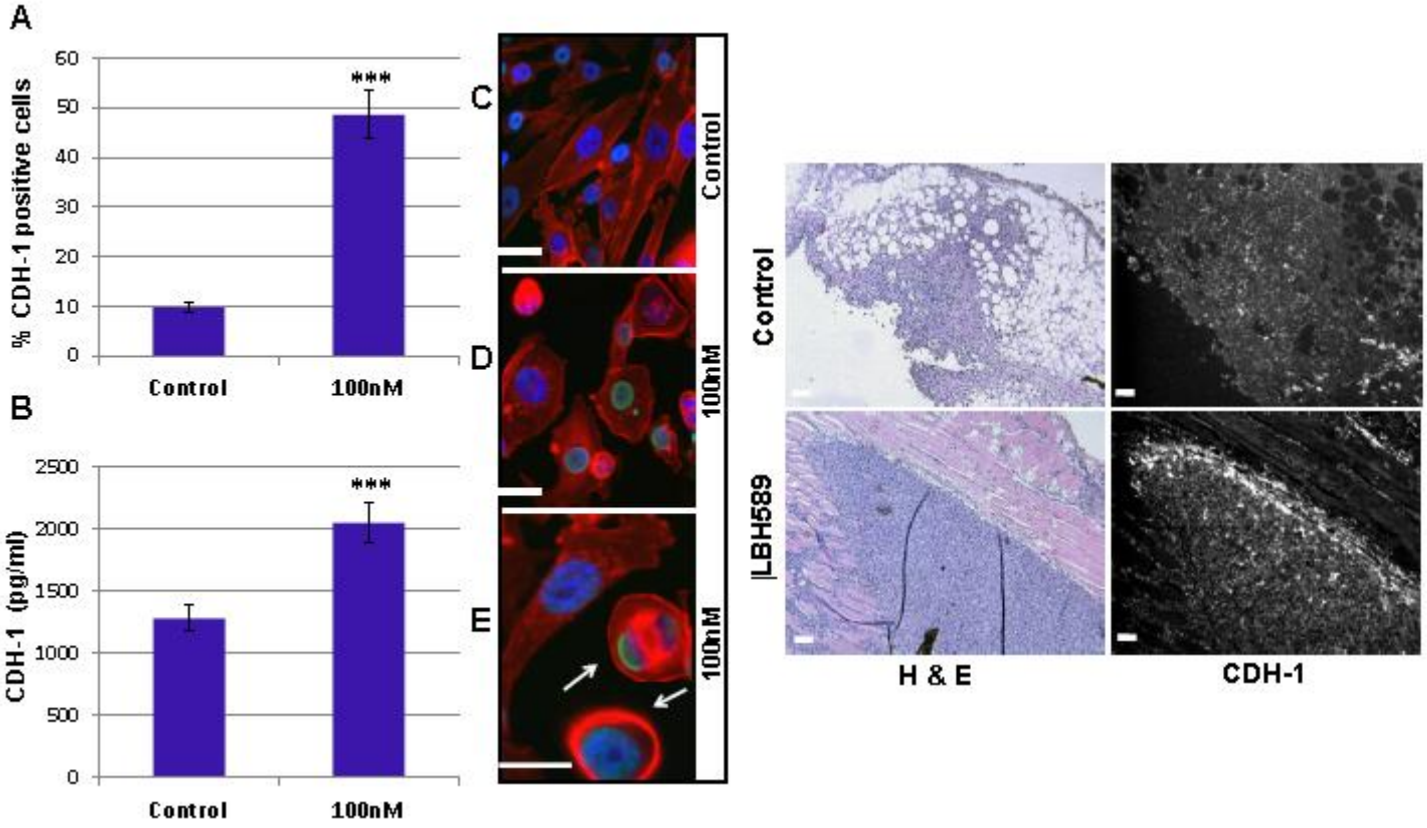

To confirm the effects previously observed that HDAC treatment inhibited cell migration in our MDA-MB-231 and MDA-MB-468 cell lines, we further tested the effects on our other TNBC lines MDA-MB-157 and BT-549. Treatment with an HDACi (100 nM) for 24hrs results in decreased migration of TNBC cell lines. Additionally, preliminary results with MDA-MB-231 cells treated with an HDACi (100 nM) for 24 hours revealed a decreased ability to invade through a matrigel coated membrane. These results are included in a manuscript currently in preparation anticipated to be submitted to *Clinical Cancer Research* titled "LBH589 inhibits metastasis in triple-negative breast cancer through regulation of microRNA and EMT" which explores the HDACi mechanism of EMT regulation.

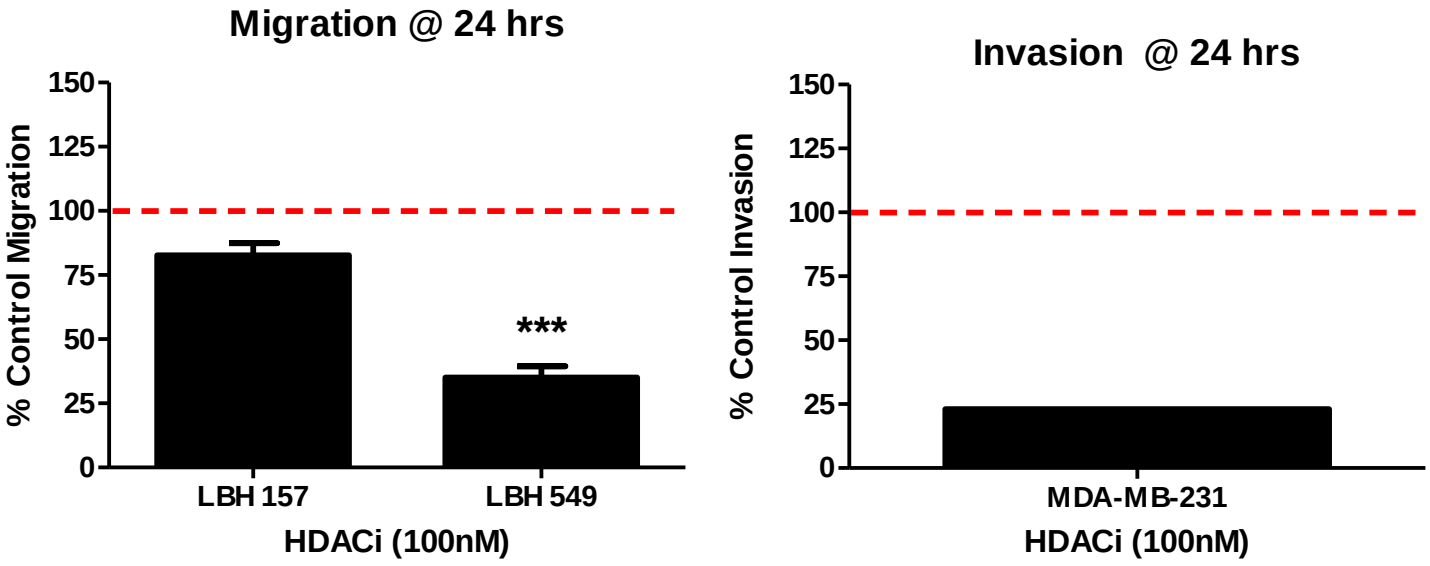

Task 3. Anti-miR strategies to reverse effects of HDACi and miR on EMT.

This task has been initiated. We have generated stable cell lines expression the following miRs in our TNBC cell lines: miRs 194, 200b, 215, and 335. Biological characterization of these cells, including analysis for effects of on EMT phenotype, are ongoing.

Task 4. miR lentiviral expression library analysis of effects on EMT-MET in triple-negative breast cancer cells.

Complete

Bt-549 cells have been transduced with a miRNA lentiviral library (miR eGFP tagged). Initial screens are ongoing to identify miRs regulating EMT-MET in TNBC. Cell samples are to be sent for sequencing next month.

Task 5. Follow up analyses for miR library screen.

The experiments outlined below are currently ongoing due to the time it took to optimize the lentiviral library screen above.

Task 5a. qPCR confirmation of miRNA expression in the library transduced TNBC cells.

Cell samples from task 4 are to be sent for sequencing next month to identify the miRs which regulate EMT-MET. Once identified, individual miRs will be transfected into TNBC cells and stable cell lines generated and confirmed by qPCR.

Task 5b. Determine effects of miR expression on TNBC EMT phenotype.

Cell lines generated in task 5a will be analyzed for effects of miR expression on proliferation, migration/invasion, and expression of epithelial and mesenchymal cell markers. These experiments are currently being conducted on the stable cell lines we have already generated from task 3 (miR-200b).

Task 5c. Validation of miR effects on target gene expression.

This task is currently ongoing. TargetScan algorithms are being used to predict targets for miR identified in the above tasks as well as those previously identified in tasks 2 and 3. The effects of miR expression on predicted targets will be tested by qPCR analysis.

KEY RESEARCH ACCOMPLISHMENTS

- Identified HDACi-induced miR changes in TNBC cell lines, many of which have been implicated in EMT and metastasis regulation.
- Demonstrated increased expression of E-cadherin in TNBC cells following treatment with HDACi, indicating the reversal of the EMT phenotype.
- Demonstrated inhibition of cell migration of TNBC cell lines treated with HDACi.

REPORTABLE OUTCOMES

Rhodes LV, Bratton MR, Zhu Y, Tilghman SL, Muir SE, Salvo VA, Tate CR, Elliott S, Nephew KP, Collins-Burow BM, and Burow ME. Effects of SDF-1–CXCR4 signaling on microRNA expression and tumorigenesis in estrogen receptor-alpha (ER-α)-positive breast cancer cells, *Experimental Cell Research* 2011, **317**: 2573–2581.

Rhodes LV, Nitschke AM, Segar HC, Martin EM, Driver JL, Elliott S, Nam SY, Li M, Nephew KP, Burow ME, and Collins-Burow BM. The histone deacetylase inhibitor trichostatin A alters microRNA expression profiles in apoptosis-resistant breast cancer cells, *Oncology Reports* 2012, **27**: 10-16.

Tate CR, Rhodes LV, Segar HC, Driver JL, Pounder FN, Burow ME, and Collins-Burow BM. Targeting triple-negative breast cancer cells with the HDAC inhibitor Panobinostat, *Breast Cancer Research*, Accepted for publication April 16th, 2012.

CONCLUSION

As triple-negative breast cancer has not benefited from the advances seen in the realm of endocrine and targeted therapy thus far, it is imperative to develop novel treatment strategies for this disease. Our results reported here have identified putative microRNAs, regulated by HDAC inhibitors, whose altered expression may play a role in the initiation of an invasive phenotype. Validation of the biological roles of these microRNAs in the regulation of EMT holds promise as therapeutic targets for the reversal of the invasive and metastatic phenotype associated with the lethality of triple-negative breast carcinoma.

REFERENCES

1. Hu Z, Fan C, Oh DS et al. The molecular portraits of breast tumors are conserved across microarray platforms. BMC Genomics 2006; **7**; 96.

2. Thiery JP, Sleeman JP: Complex networks orchestrate epithelial-mesenchymal transitions. Nature Rev Mol Cell Biol 2006; 7:131-142.

3. Hurteau GJ et al. Overexpression of the microRNA has-miR-200c leads to reduced expression of transcription factor 8 and increased expression of E-Cadherin. Cancer Research 2007; 67:(17)7972-7976.

4. PA et al. The miR-200 family and miR-205 regulate epithelial to mesenchymal transition by targeting ZEB1 and SIP1. Nature Cell Biology 2008; 10(5):593-601.

5. Scott GK et al. Rapid Alteration of MicroRNA Levels by Histone Deacetylase inhibition. Cancer Research 2006; 66(3)1277-1281.

EXPERIMENTAL CELL RESEARCH 317 (2011) 2573–2581

Available online at www.sciencedirect.com

SciVerse ScienceDirect

www.elsevier.com/locate/yexcr

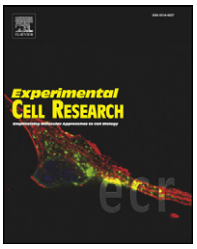

Research Article

Effects of SDF-1–CXCR4 signaling on microRNA expression and tumorigenesis in estrogen receptor-alpha (ER-α)-positive breast cancer cells

Lyndsay V. Rhodes[a,b,c], *Melyssa R. Bratton*[d], *Yun Zhu*[a,b,c], *Syreeta L. Tilghman*[e], *Shannon E. Muir*[a,b,c], *Virgilio A. Salvo*[a,b,c], *Chandra R. Tate*[a,b,c], *Steven Elliott*[a,b,c], *Kenneth P. Nephew*[h], *Bridgette M. Collins-Burow*[a,b,c,f,g], *Matthew E. Burow*[a,b,c,f,g,*]

[a] *Department of Medicine, Tulane University Health Sciences Center, 1430 Tulane Ave, New Orleans, LA 70112, USA*
[b] *Department of Section of Hematology, Tulane University Health Sciences Center, 1430 Tulane Ave, New Orleans, LA 70112, USA*
[c] *Department of Medical Oncology, Tulane University Health Sciences Center, 1430 Tulane Ave, New Orleans, LA 70112, USA*
[d] *Department of Pharmacology, Tulane University Health Sciences Center, 1430 Tulane Ave, New Orleans, LA 70112, USA*
[e] *Pulmonary Diseases Critical Care and Environmental Medicine, Tulane University Health Sciences Center, 1430 Tulane Ave, New Orleans, LA 70112, USA*
[f] *Center for Bioenvironmental Research, Tulane University Health Sciences Center, 1430 Tulane Ave, New Orleans, LA 70112, USA*
[g] *Tulane University Cancer Center, Tulane University Health Sciences Center, 1430 Tulane Ave, New Orleans, LA 70112, USA*
[h] *Medical Sciences and Department of Cellular and Integrative Physiology, Indiana University School of Medicine, Bloomington, IN 47405, USA*

ARTICLE INFORMATION

Article Chronology:
Received 21 January 2011
Revised version received
5 August 2011
Accepted 23 August 2011
Available online 30 August 2011

Keywords:
SDF-1
CXCR4
microRNA
Breast carcinoma
Hormone independence
AMD3100

ABSTRACT

The majority of breast cancer cases ultimately become unresponsive to endocrine therapies, and this progression of breast cancer from hormone-responsive to hormone-independent represents an area in need of further research. Additionally, hormone-independent carcinomas are characterized as being more aggressive and metastatic, key features of more advanced disease. Having previously shown the ability of the stromal-cell derived factor-1 (SDF-1)–CXCR4 signaling axis to promote primary tumorigenesis and hormone independence by overexpressing CXCR4 in MCF-7 cells, in this study we further examined the role of SDF-1/CXCR4 in the endogenously CXCR4-positive, estrogen receptor α (ER-α)-positive breast carcinoma cell line, MDA–MB-361. In addition to regulating estrogen-induced and hormone-independent tumor growth, CXCR4 signaling stimulated the epithelial-to-mesenchymal transition, evidenced by decreased CDH1 expression following SDF-1 treatment. Furthermore, inhibition of CXCR4 with the small molecule inhibitor AMD3100 induced CDH1 gene expression and inhibited CDH2 gene expression in MDA–MB-361 cells. Further, exogenous SDF-1 treatment induced ER-α-phosphorylation in both MDA–MB-361 and MCF-7–CXCR4 cells, demonstrating ligand-independent activation of ER-α through CXCR4 crosstalk. qPCR microRNA array analyses of the MDA–MB-361 and MCF-7–CXCR4 cell lines revealed changes in microRNA expression profiles induced by SDF-1, consistent with a more advanced disease phenotype and further supporting our hypothesis that the SDF-1/CXCR4 signaling axis drives ER-α-positive breast cancer cells to a hormone independent and more aggressive phenotype. In this first demonstration of SDF-

* *Corresponding author at:* 1430 Tulane Ave. SL-78, New Orleans, LA 70112, USA. Fax: +1 504 988 5483.
E-mail addresses: Lvanhoy@tulane.edu (L.V. Rhodes), mbratton@tulane.edu (M.R. Bratton), yun.zhu@orlandohealth.com (Y. Zhu), stilghma@xula.edu (S.L. Tilghman), shmuir@ucsd.edu (S.E. Muir), vsalvo@psm.edu (V.A. Salvo), ctate@tulane.edu (C.R. Tate), selliot@tulane.edu (S. Elliott), knephew@indiana.edu (K.P. Nephew), bcollin1@tulane.edu (B.M. Collins-Burow), mburow@tulane.edu (M.E. Burow).

0014-4827/$ – see front matter
doi:10.1016/j.yexcr.2011.08.016

1–CXCR4-induced microRNAs in breast cancer, we suggest that this signaling axis may promote tumorigenesis via microRNA regulation. These findings represent future potential therapeutic targets for the treatment of hormone-independent and endocrine-resistant breast cancer.

Introduction

Chemokines are a family of structurally related glycoproteins, originally described as molecules mediating chemotactic events [1,2]. Stromal cell-derived factor-1 (SDF-1), also known as CXCL12, is a member of the CXC chemokine subfamily and the only known ligand for CXC chemokine receptor 4 (CXCR4). Though involved in many biological processes, the SDF-1–CXCR4 signaling axis has been shown to play important roles in breast cancer [2,3]. CXCR4 is overexpressed in both primary invasive and *in situ* ductal carcinomas, suggesting an important role for the SDF-1–CXCR4 axis at all stages of the disease [4]; however, the impact of CXCR4 signaling in primary breast tumorigenesis remains to be clearly defined.

Estrogen receptor alpha (ER-α) status is a widely used prognostic marker of breast carcinoma, and it has long been known that estrogen has the ability to promote breast tumor formation and proliferation [5,6]. Inhibition of ER-α signaling abrogates the tumor promoting effects of estrogen [5,7–10]; these effects are responsible for the successful application of targeted therapies such as tamoxifen, fulvestrant (ICI 182,780), and aromatase inhibitors. Despite the effectiveness of these therapies, approximately half of ER-α-positive breast cancer patients exhibit *de novo* resistance, while those initially responsive will eventually develop resistance [11]. The progression to endocrine-resistance and hormone-independence represent hallmarks of progressive carcinoma [12,13]. We have recently demonstrated the ability of CXCR4 overexpression to promote hormone-independent tumorigenesis in the normally ER-α (+), estrogen-dependent MCF-7 breast carcinoma cell line [14]. SDF-1 is a known ER-α-mediated gene, and our data as well as others, support the existence of an ER-α–SDF-1/CXCR4 crosstalk [14,15], which may strongly contribute to the progression to hormone independence.

In addition to being overexpressed in a number of malignant cancers including breast, CXCR4 is a known mediator of metastasis [3,16–18]. The pro-metastatic effects of SDF-1/CXCR4 signaling in breast cancer can be inhibited through the use of blocking antibodies, small molecule inhibitors, as well as heparin oligosaccharides [4,14,19]. Further, SDF-1 and CXCR4 expression have been associated with the epithelial-to-mesenchymal transition (EMT) phenotype, characterized by the loss of epithelial markers (E-cadherin, Zo-1) and the gain of mesenchymal surface markers (N-cadherin, vimentin), a key step in the progression to a metastatic phenotype [14,20,21]. In addition, EMT has been shown to be regulated by microRNAs (miRNA) [22–24], small non-coding RNA (18–22 nucleotides) that downregulate the expression of target genes by degradation of mRNA or inhibition of translation [25]. Despite evidence of other chemokines mediating miRNA expression as well as miRNA targeting of chemokine signaling [26–28], the effects of SDF-1–CXCR4 signaling on miRNA expression in breast cancer have not yet been examined. This is of particular interested in the area of breast cancer research as the SDF-1–CXCR4 axis is emerging not only as a regulator of cell metastasis, but also in primary cancer tumorigenesis, hormone independence, and disease progression [4,14]. Insight into the mechanism of SDF-1–CXCR4 action in breast cancer may provide future therapeutic targets for the development of novel cancer treatments.

The purpose of this study was to investigate the effects of CXCR4 signaling on primary tumorigenesis, EMT phenotype, and regulation of ER-α phosphorylation in the endogenously ER-α (+)/CXCR4 (+) breast carcinoma cell line MDA–MB-361. To gain further mechanistic insight into the SDF-1–CXCR4 axis, we compared miRNA profiles of MDA–MB-361 cells with an MCF-7 cell line artificially overexpressing CXCR4 [14]. This is the first report of hormone-dependent and -independent regulation of MDA–MB-361 tumorigenesis by the SDF-1–CXCR4 axis and provides compelling evidence that SDF-1 induces gene, protein, and miRNA expression changes consistent with a more aggressive phenotype.

Materials and methods

Cells and reagents

The MDA–MB-361 cell line (ER-α-positive human breast cancer cell line) was acquired from ATCC. The MDA–MB-361 cell line was chosen for these studies due to their ER-α-positive status as well as high basal level expression of CXCR4 [14]. The MCF-7 cell line overexpressing CXCR4 was generated as previously published [14], and cells were cultured as previously described [29,30]. Anti-CXCR4 blocking antibody was purchased from R&D Systems (Minneapolis, MN) and AMD3100 from Sigma-Aldrich (St. Louis, MO).

Animal studies

Primary xenograft tumor studies were performed as described [29,30]. MDA–MB-361 cells were harvested and viable cells mixed with Matrigel Reduced Factors (BD Biosciences, San Jose, CA). 5×10^6 cells were injected bilaterally into the mammary fat pad of 4–6 weeks old ovariectomized female Nu/Nu mice. Tumor size was monitored by digital caliper and tumor volume calculated with the formula: $4/3\pi LM^2$ (L = larger radius, M = smaller radius). Anti-CXCR4 treatment groups were injected with cells mixed with 50ul matrigel containing anti-CXCR4 blocking antibody (75 ng/injection) or IgG control. AMD3100 treatment experiment animals were injected intraperitoneally (i.p.) with AMD3100 (5 mg/kg/animal) suspended in DMSO and PBS (1:5) once daily for the duration of the study. Specific treatment start dates are indicated in the corresponding figure legend. Experimental groups, $n = 5$. All procedures involving animals were conducted in compliance with State and Federal laws, U.S. Department of Health and Human Services, and guidelines established by Tulane University Animal Care and Use Committee. The facilities and laboratory animal programs of the University are accredited by the Association for the Assessment and Accreditation of Laboratory Animal Care.

RNA isolation and quantitative realtime PCR

Total RNA was isolated from cultured cells using RNeasy (Qiagen, Valencia, CA) following manufacturer's protocol and the quantity and quality determined by absorbance (260, 280 nm). 2 μg total RNA was reverse-transcribed (iScript kit; BioRad Laboratories, Hercules, CA) and analyzed by real-time PCR [31]. Primer sequences are as follows (Invitrogen, Carlsbad, CA): β-Actin (5′-TGAGCGCGGCTACAGCTT-3′: 5′-CCTTAATGTCACACACGATT-3′), CXCR4 (5′-GCATGACGGACAAGTACAGGCT-3′; 5′-AAAGTACCAGTTTGCCACGGC-3′), CDH1 (5;-AGGTGACAGAGCCTCTGGATAGA-3′; 5′-TGGATGACACAGCGTGAGAGA-3′), CDH2 (5;-GCCCCTCAAGTGTTACCTCAA-3′; 5′-AGCCGAGTGATGGTCCAATTT-3′), forward and reverse, respectively.

Reverse transcriptase-polymerase chain reaction

2 μg total RNA (above) was used to synthesize cDNA transcribed with SuperScript III (Invitrogen, Carlsbad, CA) and mRNA amplified. Primer sequences are as follows (Invitrogen, Carlsbad, CA): CXCR4 (5′-AGTATATACACTTCAGATAAC-3′; 5′-CCACCTTTTCAGCCAACAG-3′); SDF-1 (5′-GCCAGAGCCAACGTCAAGCATCTC-3′; 5′-GGCAAAGTGTCCAAAACAAAGCCC-3′); PgR (5′-GAATTTAGCGGGGATCCA-3′; 5′-TGCCACACTTCGATTTGT-3′); BCL2 (5′-CGCCCTGTGGATGACTGAGT-3′; 5′-GGGCCGTACAGTTCCACAA-3′); VEGF (5′-GCAGAAGGAGGAGGGCAGAATC-3′; 5′-GGCACACAGGATGGCTTGAAGATG-3′); GAPDH (5′-ACAGTCAGCCCGCATCTTCTT-3′; 5′-GACAAGCTTCCCGTTCTCAG-3′).

CDH1 ELISA

The human sE-Cadherin ELISA was carried out according to the manufacturer's protocol. Briefly, MDA–MB-361 cells (10^4 cells/well) were plated overnight and treated for 72 h with SDF-1 (100 ng/ml) or vehicle control. After cell lysis and centrifugation, the cytoplasmic fractions were diluted 1:1 with calibrator diluent and the level of E-cadherin (CDH1) determined by sE-Cadherin ELISA (DCADE0; R&D Systems, Minneapolis, MN). The absorbance was read on a Bio-Tek Synergy plate reader (Winooski, VT) at 450 nm. Data represented as mean percent control ± SEM. Assays were run in triplicate with internal duplicate drug treatments.

Western blot analysis

Western blot analyses were conducted as published [32]. After 72 h in phenol red-free DMEM medium supplemented with 5% charcoal-stripped fetal bovine serum (CS-FBS), cells were refed with medium containing SDF-1 (100 ng/ml). Cells were harvested at the indicated time points (0–120 min) in PBS/EDTA. Membranes were probed with primary antibodies according to manufacturer's protocol. Antibodies are phospho S118, phospho S167 (Cell Signaling Technology, Danvers, MA), total ER-α, Rho-GDI (Santa Cruz Biologicals, Santa Cruz, CA). IR-tagged secondary antibodies were purchased from Li-Cor Biosciences. Blots were analyzed by the Odyssey Infrared Imaging System (Li-Cor Biosciences, Lincoln, NE). Experiments were conducted in triplicate.

microRNA qPCR array

The Human Cancer microRNA RT² Profiler™ PCR Arrays (MAH-102A) were obtained from SABiosciences (Frederick, MD). MDA–MB-361 or MCF-7–CXCR4 cells were plated in 5% CS DMEM at 50% confluency and treated 24 h later with SDF-1 (100 ng/ml) or vehicle for 24 h. Cells were harvested and total RNA, including small RNA, was isolated using the miRNeasy kit per manufacturer's instructions (Qiagen, Valencia, CA). The quantity and quality of the RNA were determined by absorbance at 260 and 280 nm using the NanoDrop ND-1000 spectrophotometer (NanoDrop, Wilmington, DE). Total RNA (1.5 μg) was reverse-transcribed using the miRNA RT^2 First Strand cDNA synthesis kit following manufacturer's protocol (SABiosciences, Frederick, MD) and assayed via an optimized, real-time RT-PCR reaction for expression of 84 miRNA genes related to cancer regulation according to the manufacturer's protocol. Experiments were run in triplicate.

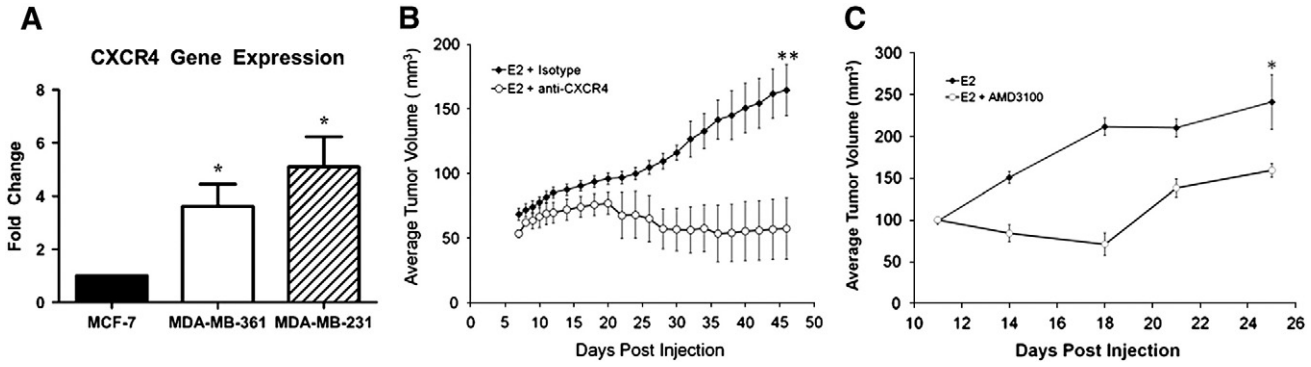

Fig. 1 – CXCR4 expression drives estrogen-stimulated MDA–MB-361 tumorigenesis. (A) MDA–MB-361 cells were harvested for RNA isolation and basal expression of CXCR4 examined by qPCR compared to MCF-7 and MDA–MB-231 cells. Bars represent mean fold expression ± SEM of triplicate experiments. (B–C) Female, 4–6 weeks old, ovariectomized Nu/Nu mice ($n = 5$/group) were injected (MFP) with 5×10^6 MDA–MB-361 cells in 50ul of Matrigel. Animals were implanted with 17β-estradiol (0.72 mg, 60 day time release) pellets subcutaneously in the dorsal neck. (B) Matrigel injections contained isotype IgG or anti-CXCR4 (75 ng/injection) antibodies. (C) Following tumor formation (11 days post cell injection), animals were treated with twice daily i.p. injections of vehicle or AMD3100 (5 mg/kg/animal). Tumors were measured by digital caliper. Data represented as average tumor volume (mm^3) ± SEM. $^*p < 0.05$, $^{**}p < 0.01$.

Statistical analysis

Studies involving >2 groups analyzed by one-way ANOVA with Tukey's post-test; all others were subjected to unpaired Student's *t*-test (Graph Pad Prism V.4). *p*-Values < 0.05 were considered statistically significant.

Results

CXCR4 signaling regulates estrogen-stimulated MDA–MB-361 tumorigenesis

CXCR4 gene expression levels were confirmed by qPCR in the MDA–MB-361 breast cancer cell line (3.62 ± 0.82 fold, $p < 0.05$) compared to the known ER-α (+)/CXCR4^{low} MCF-7 cell line (set to 1) and the ER-α (−)/CXCR4^{high} MDA–MB-231 cell line (5.09 ± 1.14 fold, $p < 0.05$) (Fig. 1A). RT-PCR analysis of cells treated with estrogen (100pM) for 18 h revealed increased levels of ER-α-mediated genes including PgR, BCL2, and VEGF-A (Supplemental Fig. 1A) confirming intact ER-α signaling in our MDA–MB-361 cell system. Additionally, SDF-1, an ER-α-inducible gene [33], was increased 4.8 ± 0.34 fold ($p < 0.001$) in response to estrogen stimulation (Supplemental Fig. 1B), further demonstrating a link between ER-α signaling and the SDF-1/CXCR4 axis.

We have previously shown that artificial CXCR4 overexpression enhances tumor growth in the ER-α-dependent MCF-7 breast carcinoma cell line [14]. Therefore, having confirmed endogenous expression of CXCR4 in the MDA–MB-361 cell line, the effects of CXCR4 signaling on MDA–MB-361 tumorigenesis were examined using our well established xenograft tumor model [14]. 4–6 week old ovariectomized female nude mice supplemented with 17β-estradiol pellets (0.72 mg, 60 day release) were injected with MDA–MB-361 cells in the mammary fat pad (MFP). Results revealed decreased estrogen-stimulated tumor volume in animals injected with MDA–MB-361 cells mixed with matrigel containing anti-CXCR4 blocking antibody (57.7 ± 23.7 mm^3, $p < 0.01$) compared to isotype control (164.8 ± 19.8 mm^3; Fig. 1B) on day 46 post cell injection, as well as animals treated with daily injections of AMD3100 (159.4 ± 19.0 mm^3, $p < 0.05$) compared to vehicle control animals (241.2 ± 37.8 mm^3; Fig. 1C) on day 25 post cell injection. These results reveal a role for SDF-1/CXCR4 signaling in hormone-driven tumorigenesis of MDA–MB-361 cells.

CXCR4 expression drives hormone-independent MDA–MB-361 tumorigenesis

Though MDA–MB-361 cells remain estrogen-responsive both *in vitro* and *in vivo*, these cells also possess the ability to grow independently of estrogen in a xenograft model (Supplemental Fig. 1C). Previous work from our lab demonstrated the ability of CXCR4 overexpression to induce hormone-independent tumorigenesis in an artificial system [14]; therefore, the effect of CXCR4 signaling on MDA–MB-361 hormone-independent tumorigenesis was also examined. 4–6 week old ovariectomized female nude mice were injected with MDA–MB-361 cells in the MFP in the absence of estrogen. Following detectable tumor formation (day 26 post cell injection), animals were randomized into treatment groups which received daily i.p. injections of the CXCR4-specific inhibitor AMD3011 (5 mg/kg) or vehicle control for 15 days. As shown in Fig. 2A, at day 41 post cell injection, tumor volume in animals treated with AMD3100 was significantly decreased (33.6 ± 7.8 mm^3, $p < 0.05$) compared to vehicle treated animals (73.6 ± 11.1 mm^3).

CXCR4 signaling promotes the epithelial-to-mesenchymal transition

The SDF-1/CXCR4 axis is a known mediator of cell migration and metastasis [1,3,34,35] and the expression of CXCR4 is correlated with decreased patient survival [14,36,37]. Furthermore, the acquisition of mesenchymal characteristics through the process known as epithelial-to-mesenchymal transition (EMT) has been

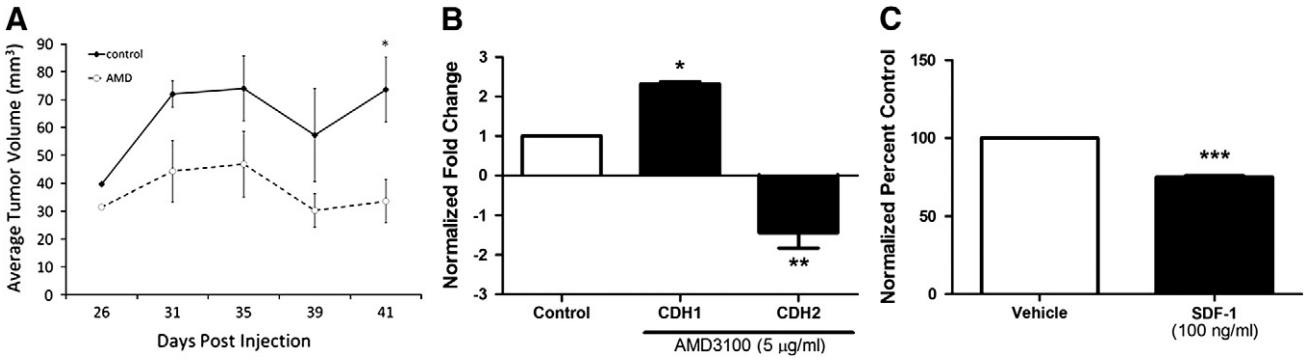

Fig. 2 – CXCR4 signaling drives MDA–MB-361 hormone-independent tumorigenesis and stimulates EMT. (A) 4–6 week old Nu/Nu ovariectomized female mice were injected (MFP) with 5×10^6 MDA–MB-361 cells mixed with matrigel (reduced factor). After tumor formation (day 26 post cell injection), animals were randomized into treatment groups and received once daily i.p. treatment with the CXCR4 inhibitor AMD3100 (5 mg/kg/animal) or vehicle control. Tumors were measured by digital caliper. Data represented as average tumor volume (mm^3) ± SEM. (B) qPCR analysis of EMT-related genes, CDH1 and CDH2, in MDA–MB-361 cells treated with AMD3100 (5 μg/ml) for 48 h. Bars represent mean fold change ± SEM of triplicate samples, vehicle normalized to 1. (C) CDH1 protein levels as detected by CDH1 ELISA of MDA–MB-361 cells treated with SDF-1 (100 ng/ml) for 72 h. Bars represent mean percent positive ± SEM of triplicate samples, vehicle normalized to 100%. $^*p < 0.05$; $^{**}p < 0.01$; $^{***}p < 0.001$.

associated with increased migration, invasion, and metastasis [38]. Therefore, we next examined the role of CXCR4 signaling on EMT-related genes by qPCR analyses. Inhibition of CXCR4 by AMD3100 (5 μgml) in MDA–MB-361 cells for 48 h resulted in increased expression of CDH1 (2.32 ± 0.05 fold, $p < 0.05$), a well known epithelial cell marker, and decreased expression of CDH2 (-1.44 ± 0.39 fold, $p < 0.01$), a mesenchymal cell marker, compared to vehicle treated cells (normalized to 1; Fig. 2B). Additionally, as illustrated in Fig. 2C, SDF-1 treatment (100 ng/ml) for 72 h was sufficient to decrease CDH1 protein expression by 25% compared to controls as determined by ELISA (from 100% to $74.94 \pm 0.9398\%$; $p < 0.001$).

SDF-1 induces ER phosphorylation and microRNA expression changes concordant with a more advanced tumor phenotype

To determine if the effects of CXCR4 signaling on hormone-independence were mediated through activation of the ER, western blot analysis for phosphorylated ER-α was conducted. Analysis of MDA–MB-361 cells (Fig. 3A) and our previously characterized MCF-7 cell line stably overexpressing CXCR4 (MCF-7–CXCR4, Fig. 3B) revealed a time-dependent increase in ER-α phosphorylation at both S118 and S167 following SDF-1 treatment (100 ng/ml). These data suggest the hormone-independent phenotype observed may be due, at least in part, to the existence of an SDF-1/CXCR4-ER-α crosstalk, in both an artificial (MCF-7–CXCR4) and an endogenous (MDA–MB-361) cell system, consistent with previous reports [14,15].

Altered miRNA expression is a common characteristic of many cancers, including breast, and their effects, both oncogenic and tumor suppressive, are exerted via regulation of many processes including tumorigenesis [39], hormone independence and endocrine resistance [40–43], EMT [44] and metastasis [45]. miRNA qPCR superarray analyses of MDA–MB-361 cells (Fig. 3C) and MCF-7–CXCR4 cells (Fig. 3D) treated with SDF-1 for 24 h revealed a number of changes in the miRNA expression compared to vehicle treated cells. Clustergrams shown in Fig. 3B–C illustrate miRNA expression changes for 3 independent samples. Table 1 displays the miRNAs found to have significantly ($p < 0.01$) changed expression in response to SDF-1 treatment (miRNAs commonly altered between both cell lines are listed first).

Discussion

CXCR4 expression is highly correlated with decreased breast carcinoma patient survival [14,36,37] and the SDF-1–CXCR4 axis is a known regulator of cancer metastasis [34–37,46,47]. Consistent with the role of CXCR4 in cancer cell proliferation, survival and metastasis, patient data now show that persons diagnosed with CXCR4(+) tumors have a significantly worse survival prognosis than those with CXCR4(−) tumors, independent of ER status [14,36]. Studies examining CXCR4 expression in clinical breast carcinoma samples revealed CXCR4 expression in both primary invasive breast carcinomas as well as ductal carcinoma *in situ* (DCIS), suggesting a role for the SDF-1–CXCR4 axis at all stages of the disease [4]. Despite numerous studies on the SDF-1–CXCR4 axis, its role in primary tumorigenesis is not fully understood. Using the endogenously CXCR4 and ER-α-positive MDA–MB-361 breast carcinoma cell line in addition to our MCF-7–CXCR4 cell line, we have shown here that inhibition of SDF-1–CXCR4 signaling reduces both hormone-independent and estrogen-induced tumorigenesis *in vivo*. Furthermore, we show the ability of SDF-1 treatment to induce phosphorylation of the ER-α at both S118 and S167, indicating ligand-independent activation, and further supporting the existence of SDF-1/CXCR4-ER-α crosstalk in the regulation of hormone-independence.

Analysis of miRNAs regulated by SDF-1 using qPCR revealed key miRNAs involved in ER-α regulation. miRNAs miR-222, miR-206, and miR-18b, miRNAs previously shown by us and others to target ER-α [48–50], were aberrantly expressed following stimulation with SDF-1. Importantly, miR-222 is not only a known repressor of ER-α gene expression, but has also been implicated in establishing resistance to both tamoxifen [51] and, more recently, fulvestrant [41]. It has been suggested that miR-222 is involved in the transition from an ER-α (+) status to an ER-α (−) one, indicative of the progression to a more advanced phenotype [49]. Furthermore, SDF-1 induced the expression of miRNAs commonly shown to be upregulated in ER-α (−) breast cancer profiles, including miR-222, miR-206, and miR-181 d [49,52]. Taken together, these data suggest that the SDF-1–CXCR4 axis mediates hormone independence and the progression to a more aggressive phenotype through mechanisms including miRNA expression changes and ER-α regulation.

While progression to hormone independence is a hallmark of advanced breast carcinomas which ultimately progress to more invasive and metastatic phenotypes [53], and the link between SDF-1/CXCR4 expression and breast cancer metastasis has been clearly documented [3,16,35], we demonstrate here that SDF-1 also stimulates the EMT, a key feature of metastatic cells, through decreased expression of the epithelial marker CDH1. Furthermore, inhibition of CXCR4 signaling with AMD3100 revealed inverse effects with increased CDH1 gene expression and decreased expression of CDH2, a mesenchymal cell marker. While the precise mechanism is currently unknown, we believe these data, along with our previously published work [14], suggest SDF-1/CXCR4 regulation of EMT.

Regulation of miRNA expression might represent one possible mechanism underlying SDF-1 regulation of EMT. qPCR miRNA analyses revealed significant SDF-1-induced changes in expression of miRs associated with the regulation of cellular invasion and metastasis. Well established metastatic-inducing miRNAs miR-214, miR-222, and miR-373 were increased following treatment with SDF-1 [54–57]. SDF-1 also upregulated miRNAs miR-143 and miR-142-5p, which have been reported to be increased in profiling studies of metastatic versus non-metastatic tumor samples [58–60]. These data suggest that altered miRNA expression may play a role in the ability of SDF-1 to induce a more mesenchymal phenotype in MDA–MB-361 and MCF-7–CXCR4 cells.

The current study demonstrates a role for SDF-1–CXCR4 signaling in both estrogen-induced and hormone-independent tumorigenesis of the endogenously CXCR4-positive, ER-α (+) breast cancer cell line MDA–MB-361. Furthermore, SDF-1 treatment induced changes in miRNA expression, demonstrated here for the first time, consistent with hormone independence and metastasis. In addition to furthering our knowledge of the role of the SDF-1–CXCR4 axis in the progression of breast carcinoma, these data provide insight into the effects of SDF-1–CXCR4 signaling on miRNA expression, a novel alternative mechanism which may provide future therapeutic targets for the treatment of ER-α (+), CXCR4 (+), hormone-independent breast disease.

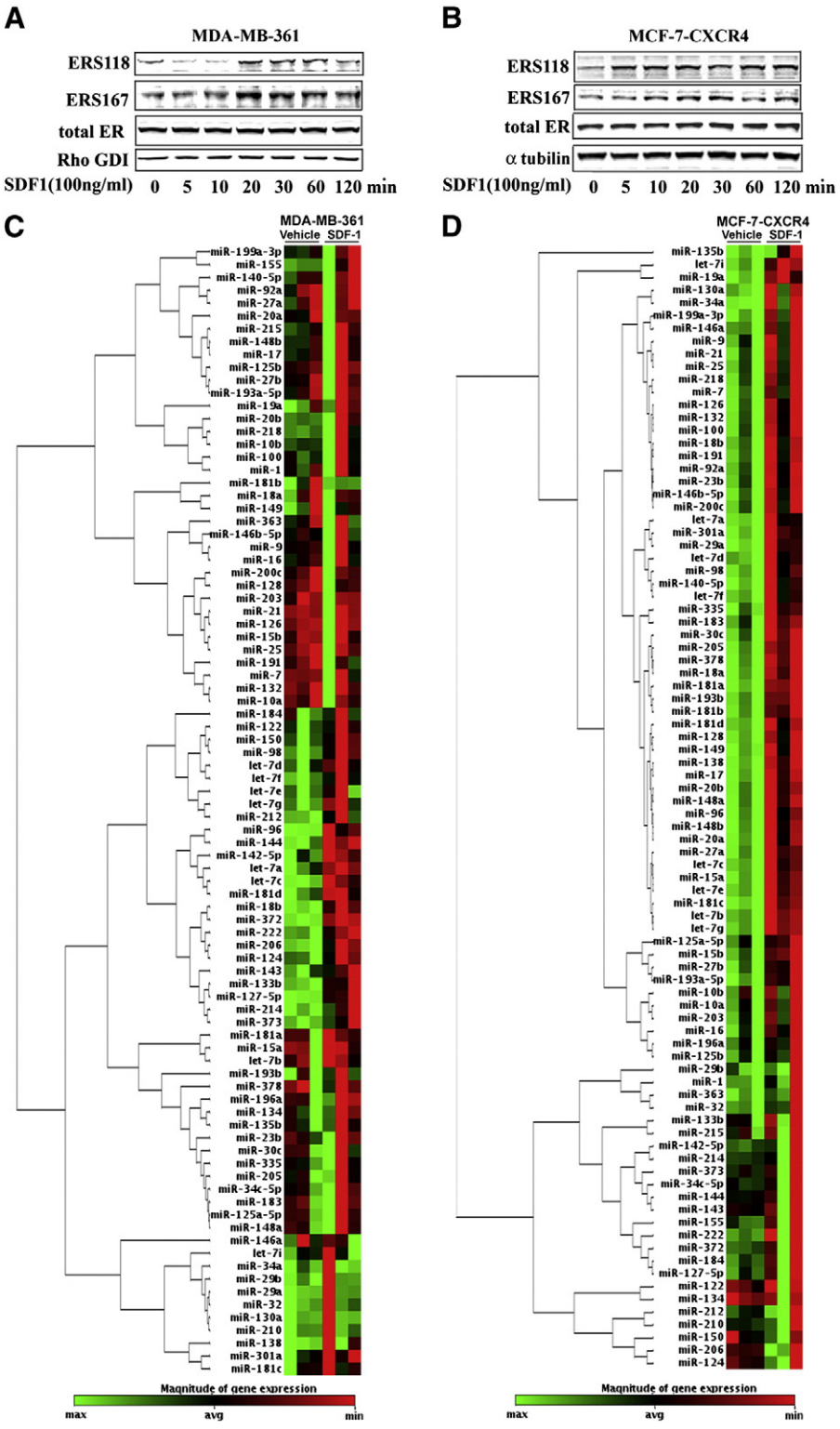

Fig. 3 – SDF-1 activates ER-α via phosphorylation and alters miR expression consistent with more advanced phenotype. (A–B) Western blot analysis for ER-α phosphorylation at serine 118 and serine 167 in a time course treatment of (A) MDA–MB-361 or (B) MCF-7–CXCR4 cells with SDF-1 (100 ng/ml) following 72 h of serum starvation. Rho GDI or α-tubulin were used as loading controls. Each gel is representative of three independent blots. (C–D) Representative clustergrams of miRNA expression changes as determined by qPCR arrays in (C) MDA–MB-361 or (D) MCF-7–CXCR4 cells following 24 h of treatment with SDF-1 (100 ng/ml). Red indicates increased expression, while green denotes decreased expression.

Table 1 – SDF-1-induced microRNA expression changes in CXCR4-positive breast carcinoma cells.

MDA–MB-361		
microRNA	Fold change	*p*-Value
18b	1.82	<0.01
96	1.39	<0.01
98	2.49	<0.05
181d	1.26	<0.05
let-7a	1.59	<0.01
let-7c	1.56	<0.01
let-7d	1.56	<0.05
let-7f	2.59	<0.05
let-7g	1.25	<0.05
124	3.14	<0.05
127-5p	1.87	<0.01
133b	4.57	<0.05
142-5p	2.12	<0.05
143	1.76	<0.05
144	5.71	<0.001
150	5.41	<0.05
206	5.91	<0.05
214	3.74	<0.05
222	1.99	<0.01
372	4.40	<0.001
373	12.61	<0.05
MCF-7–CXCR4		
microRNA	Fold change	*p*-Value
18b	1.89	<0.05
96	19.34	<0.05
98	20.53	<0.05
181d	4.54	<0.01
let-7a	24.70	<0.05
let-7c	5.23	<0.01
let-7d	2.97	<0.05
let-7f	5.71	<0.05
let-7g	15.38	<0.001
7	13.86	<0.05
15a	10.46	<0.01
15b	9.62	<0.01
16	15.67	<0.05
17	31.05	<0.01
18a	4.53	<0.01
19a	26.97	<0.01
20a	34.70	<0.01
20b	17.07	<0.01
23b	11.00	<0.05
25	8.48	<0.05
27a	28.44	<0.01
27b	16.95	<0.05
29a	44.32	<0.01
30c	15.78	<0.01
34a	2.05	<0.05
92a	3.84	<0.05
100	18.51	<0.05
126	19.84	<0.05
128	7.36	<0.05
130a	2.30	<0.05
132	7.26	<0.05
138	8.96	<0.01
140-5p	14.55	<0.05
146a	2.16	<0.05
146b-5p	7.76	<0.05
148a	23.16	<0.01
148ab	21.41	<0.01
149	5.07	<0.05
181a	3.78	<0.001
181b	6.73	<0.01
181c	3.66	<0.001
183	9.11	<0.05
191	10.13	<0.05
193a-5p	3.27	<0.01
193b	7.53	<0.01
199a-3p	3.78	<0.05
200c	9.96	<0.05
205	5.04	<0.01
218	7.13	<0.05
301a	18.29	<0.01
335	5.66	<0.05
378	9.92	<0.01
let7b	3.48	<0.001
let-7e	16.22	<0.01
let-7i	7.67	<0.01

Conflict of interest statement

The authors declare no conflicts of interest.

Supplementary materials related to this article can be found online at doi:10.1016/j.yexcr.2011.08.016.

Acknowledgments

This research was supported by Susan G. Komen Breast Cancer Foundation BCTR0601198 (ME Burow); The Department of Defense Breast Cancer Research ProgramBC061597 (LV Rhodes) and BC085426 (BM Collins-Burow); The National Institutes of Health/National Center for Research Resources P20RR020152 (BM Collins-Burow) and NCI U54 CA113001 (KP Nephew) and CA125806 (ME Burow); and The Office of Naval Research N00014-16-1-1136 (ME Burow). The funders did not have any involvement in study design; the collection, analysis, or interpretation of the data; the writing of the manuscript; or the decision to submit the manuscript for publication.

REFERENCES

[1] F. Balkwill, The significance of cancer cell expression of the chemokine receptor CXCR4, Semin. Cancer Biol. 14 (2004) 171–179.
[2] G. Lazennec, A. Richmond, Chemokines and chemokine receptors: new insights into cancer-related inflammation, Trends Mol. Med. 16 (2010) 133–144.
[3] A. Muller, B. Homey, H. Soto, N. Ge, D. Catron, M.E. Buchanan, T. McClanahan, E. Murphy, W. Yuan, S.N. Wagner, J.L. Barrera, A. Mohar, E. Verastegui, A. Zlotnik, Involvement of chemokine receptors in breast cancer metastasis, Nature 410 (2001) 50–56.
[4] M.C. Smith, K.E. Luker, J.R. Garbow, J.L. Prior, E. Jackson, D. Piwnica-Worms, G.D. Luker, CXCR4 regulates growth of both primary and metastatic breast cancer, Cancer Res. 64 (2004) 8604–8612.

[5] V.C. Jordan, M.M. Gottardis, S.P. Robinson, A. Friedl, Immune-deficient animals to study "hormone-dependent" breast and endometrial cancer, J. Steroid Biochem. 34 (1989) 169–176.
[6] S. Ali, R.C. Coombes, Estrogen receptor alpha in human breast cancer: occurrence and significance, J. Mammary Gland Biol. Neoplasia 5 (2000) 271–281.
[7] A. Brodie, G. Sabnis, D. Jelovac, Aromatase and breast cancer, J. Steroid Biochem. Mol. Biol. 102 (2006) 97–102.
[8] V.C. Jordan, Long-term tamoxifen therapy to control or to prevent breast cancer: laboratory concept to clinical trials, Prog. Clin. Biol. Res. 262 (1988) 105–123.
[9] M.J. Reed, The role of aromatase in breast tumors, Breast Cancer Res. Treat. 30 (1994) 7–17.
[10] A.E. Wakeling, J. Bowler, ICI 182,780, a new antioestrogen with clinical potential, J. Steroid Biochem. Mol. Biol. 43 (1992) 173–177.
[11] R. Clarke, M.C. Liu, K.B. Bouker, Z. Gu, R.Y. Lee, Y. Zhu, T.C. Skaar, B. Gomez, K. O'Brien, Y. Wang, L.A. Hilakivi-Clarke, Antiestrogen resistance in breast cancer and the role of estrogen receptor signaling, Oncogene 22 (2003) 7316–7339.
[12] M. Garcia, D. Derocq, G. Freiss, H. Rochefort, Activation of estrogen receptor transfected into a receptor-negative breast cancer cell line decreases the metastatic and invasive potential of the cells, Proc. Natl. Acad. Sci. U. S. A. 89 (1992) 11538–11542.
[13] T. van Agthoven, A.M. Sieuwerts, M.E. Meijer-van Gelder, M.P. Look, M. Smid, J. Veldscholte, S. Sleijfer, J.A. Foekens, L.C. Dorssers, Relevance of breast cancer antiestrogen resistance genes in human breast cancer progression and tamoxifen resistance, J. Clin. Oncol. 27 (2009) 542–549.
[14] L.V. Rhodes, S.P. Short, N. Neel, V.A. Salvo, Y. Zhu, S. Elliott, Y. Wei, D. Yu, M. Sun, S.E. Muir, J.P. Fonseca, M.R. Bratton, C. Segar, S.L. Tilghman, T. Sobolik-Delmaire, L.W. Horton, S. Zaja-Milatovic, B.M. Collins-Burow, S. Wadsworth, B.S. Beckman, C.E. Wood, S.A. Fuqua, K.P. Nephew, P. Dent, R.A. Worthylake, T.J. Curiel, M.C. Hung, A. Richmond, M.E. Burow, Cytokine receptor CXCR4 mediates estrogen-independent tumorigenesis, metastasis, and resistance to endocrine therapy in human breast cancer, Cancer Res. 71 (2) (2010) 603–613.
[15] K. Sauve, J. Lepage, M. Sanchez, N. Heveker, A. Tremblay, Positive feedback activation of estrogen receptors by the CXCL12–CXCR4 pathway, Cancer Res. 69 (2009) 5793–5800.
[16] M. Darash-Yahana, E. Pikarsky, R. Abramovitch, E. Zeira, B. Pal, R. Karplus, K. Beider, S. Avniel, S. Kasem, E. Galun, A. Peled, Role of high expression levels of CXCR4 in tumor growth, vascularization, and metastasis, FASEB J. 18 (2004) 1240–1242.
[17] S. Hirakawa, M. Detmar, D. Kerjaschki, S. Nagamatsu, K. Matsuo, A. Tanemura, N. Kamata, K. Higashikawa, H. Okazaki, K. Kameda, H. Nishida-Fukuda, H. Mori, Y. Hanakawa, K. Sayama, Y. Shirakata, M. Tohyama, S. Tokumaru, I. Katayama, K. Hashimoto, Nodal lymphangiogenesis and metastasis: role of tumor-induced lymphatic vessel activation in extramammary Paget's disease, Am. J. Pathol. 175 (2009) 2235–2248.
[18] A. Orimo, P.B. Gupta, D.C. Sgroi, F. Arenzana-Seisdedos, T. Delaunay, R. Naeem, V.J. Carey, A.L. Richardson, R.A. Weinberg, Stromal fibroblasts present in invasive human breast carcinomas promote tumor growth and angiogenesis through elevated SDF-1/CXCL12 secretion, Cell 121 (2005) 335–348.
[19] P. Mellor, J.R. Harvey, K.J. Murphy, D. Pye, G. O'Boyle, T.W. Lennard, J.A. Kirby, S. Ali, Modulatory effects of heparin and short-length oligosaccharides of heparin on the metastasis and growth of LMD MDA–MB 231 breast cancer cells in vivo, Br. J. Cancer 97 (2007) 761–768.
[20] A.M. Fischer, J.C. Mercer, A. Iyer, M.J. Ragin, A. August, Regulation of CXC chemokine receptor 4-mediated migration by the Tec family tyrosine kinase ITK, J. Biol. Chem. 279 (2004) 29816–29820.
[21] T. Onoue, D. Uchida, N.M. Begum, Y. Tomizuka, H. Yoshida, M. Sato, Epithelial-mesenchymal transition induced by the stromal cell-derived factor-1/CXCR4 system in oral squamous cell carcinoma cells, Int. J. Oncol. 29 (2006) 1133–1138.
[22] L. Ma, R.A. Weinberg, MicroRNAs in malignant progression, Cell Cycle 7 (2008) 570–572.
[23] C.P. Bracken, P.A. Gregory, Y. Khew-Goodall, G.J. Goodall, The role of microRNAs in metastasis and epithelial–mesenchymal transition, Cell. Mol. Life Sci. 66 (2009) 1682–1699.
[24] P.A. Gregory, C.P. Bracken, A.G. Bert, G.J. Goodall, MicroRNAs as regulators of epithelial–mesenchymal transition, Cell Cycle 7 (2008) 3112–3118.
[25] V. Ambros, microRNAs: tiny regulators with great potential, Cell 107 (2001) 823–826.
[26] M.M. Perry, A.E. Williams, E. Tsitsiou, H.M. Larner-Svensson, M.A. Lindsay, Divergent intracellular pathways regulate interleukin-1beta-induced miR-146a and miR-146b expression and chemokine release in human alveolar epithelial cells, FEBS Lett. 583 (2009) 3349–3355.
[27] T. Xia, A. O'Hara, I. Araujo, J. Barreto, E. Carvalho, J.B. Sapucaia, J.C. Ramos, E. Luz, C. Pedroso, M. Manrique, N.L. Toomey, C. Brites, D.P. Dittmer, W.J. Harrington Jr., EBV microRNAs in primary lymphomas and targeting of CXCL-11 by ebv-mir-BHRF1-3, Cancer Res. 68 (2008) 1436–1442.
[28] X. Zhao, Y. Tang, B. Qu, H. Cui, S. Wang, L. Wang, X. Luo, X. Huang, J. Li, S. Chen, N. Shen, MicroRNA-125a contributes to elevated inflammatory chemokine RANTES via targeting KLF13 in systemic lupus erythematosus, Arthritis Rheum. 62 (11) (2010) 3425–3435.
[29] L.V. Rhodes, S.E. Muir, S. Elliott, L.M. Guillot, J.W. Antoon, P. Penfornis, S.L. Tilghman, V.A. Salvo, J.P. Fonseca, M.R. Lacey, B.S. Beckman, J.A. McLachlan, B.G. Rowan, R. Pochampally, M.E. Burow, Adult human mesenchymal stem cells enhance breast tumorigenesis and promote hormone independence, Breast Cancer Res. Treat. 121 (2010) 293–300.
[30] V.A. Salvo, S.M. Boue, J.P. Fonseca, S. Elliott, C. Corbitt, B.M. Collins-Burow, T.J. Curiel, S.K. Srivastav, B.Y. Shih, C. Carter-Wientjes, C.E. Wood, P.W. Erhardt, B.S. Beckman, J.A. McLachlan, T.E. Cleveland, M.E. Burow, Antiestrogenic glyceollins suppress human breast and ovarian carcinoma tumorigenesis, Clin. Cancer Res. 12 (2006) 7159–7164.
[31] M.C. Zimmermann, S.L. Tilghman, S.M. Boue, V.A. Salvo, S. Elliott, K.Y. Williams, E.V. Skripnikova, H. Ashe, F. Payton-Stewart, L. Vanhoy-Rhodes, J.P. Fonseca, C. Corbitt, B.M. Collins-Burow, M.H. Howell, M. Lacey, B.Y. Shih, C. Carter-Wientjes, T.E. Cleveland, J.A. McLachlan, T.E. Wiese, B.S. Beckman, M.E. Burow, Glyceollin I, a novel antiestrogenic phytoalexin isolated from activated soy, J. Pharmacol. Exp. Ther. 332 (2010) 35–45.
[32] F. Payton-Stewart, N.W. Schoene, Y.S. Kim, M.E. Burow, T.E. Cleveland, S.M. Boue, T.T. Wang, Molecular effects of soy phytoalexin glyceollins in human prostate cancer cells LNCaP, Mol. Carcinog. 48 (2009) 862–871.
[33] J.M. Hall, K.S. Korach, Stromal cell-derived factor 1, a novel target of estrogen receptor action, mediates the mitogenic effects of estradiol in ovarian and breast cancer cells, Mol. Endocrinol. 17 (2003) 792–803.
[34] M. Kato, J. Kitayama, S. Kazama, H. Nagawa, Expression pattern of CXC chemokine receptor-4 is correlated with lymph node metastasis in human invasive ductal carcinoma, Breast Cancer Res. 5 (2003) R144–R150.
[35] M.M. Richert, K.S. Vaidya, C.N. Mills, D. Wong, W. Korz, D.R. Hurst, D.R. Welch, Inhibition of CXCR4 by CTCE-9908 inhibits breast cancer metastasis to lung and bone, Oncol. Rep. 21 (2009) 761–767.
[36] N.T. Holm, F. Abreo, L.W. Johnson, B.D. Li, Q.D. Chu, Elevated chemokine receptor CXCR4 expression in primary tumors following neoadjuvant chemotherapy predicts poor outcomes for patients with locally advanced breast cancer (LABC), Breast Cancer Res. Treat. 113 (2009) 293–299.
[37] O. Salvucci, A. Bouchard, A. Baccarelli, J. Deschenes, G. Sauter, R. Simon, R. Bianchi, M. Basik, The role of CXCR4 receptor expression in breast cancer: a large tissue microarray study, Breast Cancer Res. Treat. 97 (2006) 275–283.

[38] D.S. Micalizzi, S.M. Farabaugh, H.L. Ford, Epithelial-mesenchymal transition in cancer: parallels between normal development and tumor progression, J. Mammary Gland Biol. Neoplasia 15 (2010) 117–134.
[39] E. O'Day, A. Lal, MicroRNAs and their target gene networks in breast cancer, Breast Cancer Res. 12 (2010) 201.
[40] D.M. Cittelly, P.M. Das, V.A. Salvo, J.P. Fonseca, M.E. Burow, F.E. Jones, Oncogenic HER2{Delta}16 suppresses miR-15a/16 and deregulates BCL-2 to promote endocrine resistance of breast tumors, Carcinogenesis 31 (2010) 2049–2057.
[41] X. Rao, G. Di Leva, M. Li, F. Fang, C. Devlin, C. Hartman-Frey, M.E. Burow, M. Ivan, C.M. Croce, K.P. Nephew, MicroRNA-221/222 confers breast cancer fulvestrant resistance by regulating multiple signaling pathways, Oncogene 30 (9) (2011) 1082–1097.
[42] M. Sachdeva, H. Wu, P. Ru, L. Hwang, V. Trieu, Y.Y. Mo, MicroRNA-101-mediated Akt activation and estrogen-independent growth, Oncogene 30 (7) (2011) 822–831.
[43] C. Swanton, Z. Szallasi, J.D. Brenton, J. Downward, Functional genomic analysis of drug sensitivity pathways to guide adjuvant strategies in breast cancer, Breast Cancer Res. 10 (2008) 214.
[44] J.A. Wright, J.K. Richer, G.J. Goodall, microRNAs and EMT in mammary cells and breast cancer, J. Mammary Gland Biol. Neoplasia 15 (2010) 213–223.
[45] D.R. Hurst, M.D. Edmonds, D.R. Welch, Metastamir: the field of metastasis-regulatory microRNA is spreading, Cancer Res. 69 (2009) 7495–7498.
[46] A. Krohn, Y.H. Song, F. Muehlberg, L. Droll, C. Beckmann, E. Alt, CXCR4 receptor positive spheroid forming cells are responsible for tumor invasion in vitro, Cancer Lett. 208 (2009) 65–71.
[47] W. Zhou, Z. Jiang, N. Liu, F. Xu, P. Wen, Y. Liu, W. Zhong, X. Song, X. Chang, X. Zhang, G. Wei, J. Yu, Down-regulation of CXCL12 mRNA expression by promoter hypermethylation and its association with metastatic progression in human breast carcinomas, J. Cancer Res. Clin. Oncol. 135 (2009) 91–102.
[48] B.D. Adams, H. Furneaux, B.A. White, The micro-ribonucleic acid (miRNA) miR-206 targets the human estrogen receptor-alpha (ERalpha) and represses ERalpha messenger RNA and protein expression in breast cancer cell lines, Mol. Endocrinol. 21 (2007) 1132–1147.
[49] G. Di Leva, P. Gasparini, C. Piovan, A. Ngankeu, M. Garofalo, C. Taccioli, M.V. Iorio, M. Li, S. Volinia, H. Alder, T. Nakamura, G. Nuovo, Y. Liu, K.P. Nephew, C.M. Croce, MicroRNA cluster 221–222 and estrogen receptor alpha interactions in breast cancer, J. Natl. Cancer Inst. 102 (2010) 706–721.
[50] N. Kondo, T. Toyama, H. Sugiura, Y. Fujii, H. Yamashita, miR-206 Expression is down-regulated in estrogen receptor alpha-positive human breast cancer, Cancer Res. 68 (2008) 5004–5008.
[51] T.E. Miller, K. Ghoshal, B. Ramaswamy, S. Roy, J. Datta, C.L. Shapiro, S. Jacob, S. Majumder, MicroRNA-221/222 confers tamoxifen resistance in breast cancer by targeting p27Kip1, J. Biol. Chem. 283 (2008) 29897–29903.
[52] L.X. Yan, X.F. Huang, Q. Shao, M.Y. Huang, L. Deng, Q.L. Wu, Y.X. Zeng, J.Y. Shao, MicroRNA miR-21 overexpression in human breast cancer is associated with advanced clinical stage, lymph node metastasis and patient poor prognosis, RNA 14 (2008) 2348–2360.
[53] F. Leonessa, V. Boulay, A. Wright, E.W. Thompson, N. Brunner, R. Clarke, The biology of breast tumor progression. Acquisition of hormone independence and resistance to cytotoxic drugs, Acta Oncol. 31 (1992) 115–123.
[54] M. Bar-Eli, Searching for the 'melano-miRs': miR-214 drives melanoma metastasis, EMBO J. 30 (2011) 1880–1881.
[55] N.M. White, E. Fatoohi, M. Metias, K. Jung, C. Stephan, G.M. Yousef, Metastamirs: a stepping stone towards improved cancer management, Nat. Rev. Clin. Oncol. 8 (2011) 75–84.
[56] Q. Huang, K. Gumireddy, M. Schrier, C. le Sage, R. Nagel, S. Nair, D.A. Egan, A. Li, G. Huang, A.J. Klein-Szanto, P.A. Gimotty, D. Katsaros, G. Coukos, L. Zhang, E. Pure, R. Agami, The microRNAs miR-373 and miR-520c promote tumour invasion and metastasis, Nat. Cell Biol. 10 (2008) 202–210.
[57] X. Liu, J. Yu, L. Jiang, A. Wang, F. Shi, H. Ye, X. Zhou, MicroRNA-222 regulates cell invasion by targeting matrix metalloproteinase 1 (MMP1) and manganese superoxide dismutase 2 (SOD2) in tongue squamous cell carcinoma cell lines, CANCER GENOMICS PROTEOMICS 6 (2009) 131–139.
[58] X. Peng, W. Guo, T. Liu, X. Wang, X. Tu, D. Xiong, S. Chen, Y. Lai, H. Du, G. Chen, G. Liu, Y. Tang, S. Huang, X. Zou, Identification of miRs-143 and -145 that is associated with bone metastasis of prostate cancer and involved in the regulation of EMT, PloS One 6 (2011) e20341.
[59] M. Osaki, F. Takeshita, Y. Sugimoto, N. Kosaka, Y. Yamamoto, Y. Yoshioka, E. Kobayashi, T. Yamada, A. Kawai, T. Inoue, H. Ito, M. Oshimura, T. Ochiya, MicroRNA-143 regulates human osteosarcoma metastasis by regulating matrix metalloprotease-13 expression, Mol. Ther. 19 (2011) 1123–1130.
[60] X. Zhang, S. Liu, T. Hu, Y. He, S. Sun, Up-regulated microRNA-143 transcribed by nuclear factor kappa B enhances hepatocarcinoma metastasis by repressing fibronectin expression, Hepatology 50 (2009) 490–499.

The histone deacetylase inhibitor trichostatin A alters microRNA expression profiles in apoptosis-resistant breast cancer cells

LYNDSAY V. RHODES[1], ASHLEY M. NITSCHKE[1], H. CHRIS SEGAR[1], ELIZABETH C. MARTIN[1], JENNIFER L. DRIVER[1], STEVEN ELLIOTT[1], SEUNG YOON NAM[6], MENG LI[6], KENNETH P. NEPHEW[6], MATTHEW E. BUROW[1,2,4,5] and BRIDGETTE M. COLLINS-BUROW[1,4,5]

Departments of [1]Medicine, Section of Hematology and Medical Oncology, [2]Pharmacology and [3]Pathology and Laboratory Medicine, [4]Center for Bioenvironmental Research, [5]Tulane Cancer Center, Tulane University Health Sciences Center, New Orleans, LA 70112; [6]Medical Sciences and Department of Cellular and Integrative Physiology, Indiana University School of Medicine, Bloomington, IN 47405, USA

Received July 13, 2011; Accepted August 29, 2011

DOI: 10.3892/or.2011.1488

Abstract. The development of drug resistance represents a major complication in the effective treatment of breast cancer. Epigenetic therapy, through the use of histone deacetylase inhibitors (HDACi) or demethylation agents, is an emerging area of therapeutic targeting in a number of ontological entities, particularly in the setting of aggressive therapy-resistant disease. Using the well-described HDAC inhibitor trichostatin A (TSA) we demonstrate the suppression of *in vitro* clonogenicity in the previously described apoptosis-resistant MCF-7TN-R breast carcinoma cell line. Additionally, recent work has demonstrated that these agents can alter the expression profile of microRNA signatures in malignant cells. Using an unbiased microRNA microarray analysis, changes in miRNA expression of MCF-7TN-R cells treated with TSA for 24 h were analyzed. We observed significant up-regulation of 22 miRNAs and down-regulation of 10 miRNAs in response to TSA treatment. Our results demonstrate that the HDACi, TSA, exerts anticancer activity in the apoptosis-resistant MCF-7TN-R breast carcinoma cell line. This activity is correlated with TSA alteration of microRNA expression profiles indicative of a less aggressive phenotype.

Introduction

Despite significant advancement in the area of endocrine therapies and chemotherapeutics, nearly half of breast cancer patients exhibit *de novo* resistance, while the majority of remaining patients ultimately progress to drug resistance (1). Drug resistant breast cancer is associated with poor prognoses (2,3), highlighting the critical need to develop novel therapeutics that are effective against these more aggressive forms of the disease. Epigenetic alterations, including aberrant DNA methylation and histone deacetylation, participate in cancer development and progression (4). Epigenetic aberrations lead to breast cancer chemotherapy resistance (5,6); hence, their reversal by inhibitors of DNA methylation and histone deacetylases (DNMTi and HDACi) may overcome it and are at present undergoing clinical testing, either alone or in combination with conventional chemotherapies (7).

Histone deacetylases (HDACs) and histone acetyltransferases (HATs) have important roles in the maintenance and function of chromatin by regulating the acetylation of histones. In addition, these enzymes have recently been shown to regulate the acetylation of many non-histone targets and therefore may represent a key means of post-translational regulation beyond their established roles in transcriptional regulation. The use of HDACi in the clinical setting is currently FDA-approved only for the treatment of progressive or recurrent cutaneous T-cell lymphoma following two other systemic therapies (8). Biologically, HDACi induce growth arrest, differentiation and cell death in breast cancer cells, but the underlying mechanism warrants further investigation.

In addition to direct regulation of mRNA gene expression, HDACis have been shown to alter microRNA (miRNA) expression in several human carcinomas including pancreatic (9), colon (10,11), gastric (12) and breast (13). microRNAs are small non-coding RNAs (18-22 nt) which function as an additional layer of regulation of mRNA stability and translation through 3'-UTR targeting (14). Through their ability to target the 3'-UTR of multiple genes, individual miRNAs can exert vast effects on mRNA-protein expression in cells. In cancer, miRNAs can function as tumor suppressors or oncogenes (15). We examined the effects of the HDACi trichostatin A (TSA) on the survival of the apoptotic-resistant MCF-7TN-R breast carcinoma cell line, as well as its effects on miRNA expression.

Correspondence to: Dr Bridgette M. Collins-Burow, Tulane University Health Sciences Center, Department of Medicine, 1430 Tulane Ave. SL-78, New Orleans, LA 70112, USA
E-mail: bcollin1@tulane.edu

Key words: microRNA, trichostatin A, histone deacetylase, MCF-7, breast cancer, drug resistance

Table I. microRNA microarray results for MCF-7TN-R cells treated with TSA (10 μM) for 24 h.

ID	Serial no.	Average (TSA)	Average (DMSO)	p-value	logFC
hsa-miR-215	990	498.33	323.67	0.001	1.46
hsa-miR-657	725	206.33	573.67	0.002	-1.13
hsa-miR-139	524	886.33	783.67	0.003	0.88
hsa-miR-155	544	192.67	176.33	0.005	0.73
hsa-miR-146b	1501	182.67	178.00	0.005	0.66
hsa-miR-645	1681	181.33	519.67	0.006	-1.27
hsa-miR-544	127	374.67	305.67	0.006	1.01
hsa-miR-194	1541	362.67	319.67	0.007	0.95
hsa-miR-628	696	190.67	371.67	0.007	-0.60
hsa-miR-144	1498	148.00	115.33	0.008	0.94
hsa-miR-144	530	154.67	110.67	0.008	1.10
hsa-miR-559	1112	128.67	111.67	0.008	0.74
hsa-miR-128b	511	868.00	905.00	0.009	0.62
hsa-miR-143	529	204.67	143.67	0.009	1.13
hsa-miR-568	1121	145.67	130.33	0.009	0.74
hsa-miR-769-5p	744	230.33	502.33	0.010	-0.69
hsa-miR-1	1461	226.00	130.33	0.010	1.48
hsa-miR-497	645	296.67	639.67	0.011	-0.66
hsa-miR-632	1668	217.33	603.00	0.012	-1.12
hsa-miR-767-5p	1708	178.00	392.67	0.012	-0.73
hsa-miR-512-3p	660	155.33	362.67	0.013	-0.82
hsa-miR-191*	1537	206.67	138.33	0.014	1.25
hsa-miR-191*	569	285.33	155.33	0.015	1.65
hsa-miR-155	1512	163.67	150.67	0.015	0.70
hsa-miR-613	1649	246.00	624.33	0.016	-0.93
hsa-miR-202*	977	479.33	378.00	0.016	1.05
hsa-miR-636	704	226.67	705.33	0.018	-1.20
hsa-miR-486	1600	192.00	129.67	0.019	1.21
hsa-miR-622	1658	181.33	401.67	0.019	-0.79
hsa-miR-215	22	469.00	289.00	0.020	1.61
hsa-miR-22	27	1007.33	568.33	0.021	1.82
hsa-miR-875-5p	903	139.67	103.33	0.024	0.99
hsa-miR-620	1656	210.00	127.33	0.024	1.36
hsa-miR-370	581	1265.67	1152.67	0.026	0.88
hsa-miR-200c	7	272.67	278.00	0.026	0.60
hsa-miR-638	706	1096.67	1021.00	0.026	0.85
hsa-miR-630	1666	140.33	129.00	0.028	0.71
hsa-miR-208	14	191.33	168.67	0.028	0.74
hsa-miR-526c	121	321.33	215.33	0.028	1.27
hsa-miR-643	711	138.33	268.33	0.029	-0.61
hsa-miR-651	719	142.33	332.67	0.029	-0.84
hsa-miR-149	537	733.67	711.00	0.031	0.71
hsa-miR-589	1880	150.67	137.00	0.032	0.77
hsa-miR-768-3p	1709	994.33	1006.00	0.033	0.79
hsa-miR-22	995	935.67	635.00	0.035	1.65
hsa-miR-627	1663	133.67	102.00	0.035	0.96
hsa-miR-450	1588	270.67	571.33	0.036	-0.63
hsa-miR-620	688	198.33	136.67	0.036	1.17
hsa-miR-211	987	618.67	578.33	0.037	0.83
hsa-miR-346	84	625.33	604.67	0.041	0.77

Table I. Continued.

ID	Serial no.	Average (TSA)	Average (DMSO)	p-value	logFC
hsa-miR-1	493	256.00	184.67	0.041	1.11
hsa-miR-607	191	171.33	155.33	0.041	0.70
hsa-miR-153	1509	145.67	124.00	0.041	0.85
hsa-miR-621	1657	277.00	196.00	0.042	1.10
hsa-miR-668	1700	233.33	538.67	0.043	-0.74
hsa-miR-607	1159	105.33	254.00	0.043	-1.04
hsa-miR-129	1480	533.33	495.00	0.045	0.82
hsa-miR-335	76	175.67	134.00	0.045	0.96
hsa-miR-640	1676	188.67	447.00	0.047	-0.80
hsa-miR-524*	116	256.00	243.00	0.048	0.61
hsa-miR-663	731	681.33	757.67	0.049	0.60

Materials and methods

Cell generation and culture. The apoptotic-resistant MCF-7TN-R cells were derived from MCF-7 cells grown in increasing concentrations of tumor necrosis factor α (TNFα) until resistance was established. Cells were maintained in Dulbecco's modified Eagle's medium (DMEM) (Gibco) supplemented with 10% fetal bovine serum (FBS) (10% DMEM). The detailed methods are described by Weldon *et al* (16).

Clonogenicity assay. Colony survival assays were performed as previously published (17). Briefly, cells were cultured in 10% FBS-DMEM media. Cells were seeded at a density of 2,000 cells/well in 2 ml of media in 6-well plates. Cells were allowed to adhere overnight at 37˚C and treated on the following day with vehicle (DMSO) or TSA (0.1, 1, 10 μM). After 10 days, media was removed and the cells were fixed with gluteraldehyde. Cells were stained with crystal violet (0.1% in 20% methanol) for visualization. Colonies >50 cells were manually counted and treatments normalized to vehicle control. Assays were run in quadruplicate with internal duplicates.

microRNA microarray analysis. MCF-7TN-R cells were plated at a density of $2x10^6$ cells in 25 cm^2 flasks in normal culture media (DMEM media supplemented with 5% FBS, 1% penicillin/streptomycin, 1% essential amino acids, 1% non-essential amino acids and 1% sodium pyruvate) and allowed to adhere overnight at 37˚C, 5% CO_2 and air. The following day the media was changed to phenol red-free media (supplemented as above) and 5% charcoal-stripped serum was substituted for the 5% FBS. Cells were treated with TSA (10 μM) or DMSO for 24 h. Cells were harvested in PBS, collected by centrifugation, and total RNA extracted using the miRNeasy kit (Qiagen) according to manufacturer's protocol. Enrichment for miRNA was not performed. Quantity and quality of RNA was determined by absorbance (260, 280 nm), and 5 μg total RNA was used for microarray analysis. Microarray analysis was performed as we have previously described (18). Briefly, a custom microarray (19) was used to determine miRNA expression, using three biological replicates for each condition (± TSA). Low intensity probes (signal <100 in more than half samples) were excluded from the analysis. Raw data was log-transformed and normalized by IQR. Clustering of miRNA expression data was performed using CLUSTER (20), with filtering to remove inconsistencies between replicates. For clustering, we first log-transformed the data and median-centered the array and genes, followed by average linkage clustering. Clustering results were visualized by TreeView (http://rana.lbl.gov/EisenSoftware.htm). Full array data is shown in Table I.

Statistical analyses. Colony assays were analyzed by one-way ANOVA with the Tukey's post-test (Graph Pad Prism V.4); $p<0.05$ was considered to indicate statistically significant differences. The Student's t-test was performed to evaluate the statistical significance of the cluster selection. For microRNA microarray data, the Welch's t-test was performed for each probe using their normalized signals, with p-values <0.05 considered significant as previously described (21).

Results

TSA inhibits drug-resistant breast cancer cell clonogenic survival. We have previously described the generation of the MCF-7TN-R cells (16) which have acquired resistance to TNFα- and TRAIL-induced cell death. These cells have been characterized as highly aggressive and metastatic, and have been developed as a model system of chemoresistant breast carcinoma (22,23). To determine the effects of HDACi on apoptotic and clonogenic survival, MCF-7TN-R cells were treated with varying concentrations of TSA (0.1, 1 and 10 μM) or vehicle control (DMSO) for 10 days. MCF-7TN-R cells treated with TSA at 10 μM for 10 days demonstrated a decrease ($p<0.01$) in colony formation compared to vehicle-treated cells (62.37±6.45%, Fig. 1).

TSA induces microRNA expression in MCF-7TN-R cells indicative of tumor suppressive and anti-metastatic effects. In human breast cancer, we and others have shown that specific miRNAs are significantly altered, as compared with normal breast tissue (21,24-26). Altered expression of specific miRNAs has been associated with poor prognosis (27), as well as breast cancer initiation, invasion and metastasis (28-31).

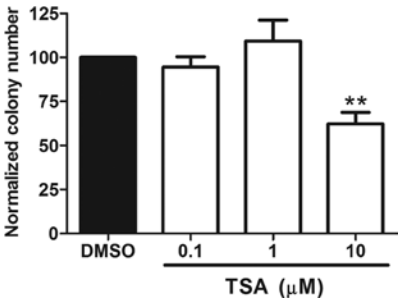

Figure 1. TSA suppression of MCF-7TN-R cell clonogenic survival. MCF-7TN-R cells were plated (2,000 cells/well) in 10% DMEM in 6-well plates and allowed to adhere overnight. Twenty-four hours later the cells were treated with vehicle (DMSO) or TSA (0.1, 1, 10 μM) for 10 days. Colonies of ≥50 cells were counted as positive. Bars represent mean percentage clonogenic survival normalized to DMSO control cells ± SEM. (**p<0.01).

The importance of miRNAs in these advanced breast cancer phenotypes raises the question of their further involvement in apoptotic resistance. Furthermore, based on the above result demonstrating MCF-7TN-R growth-inhibition by TSA, we performed microRNA microarray analysis of MCF-7TN-R cells after treatment with TSA (10 μM for 24 h). As shown in Fig. 2, a number of microRNA expression changes were observed. In addition, the three biological replicates from vehicle-treated MCF-7TN-R clustered together and separately from TSA-treated cells, demonstrating high reproducibility between biological repeats as well as differential microRNA expression induced by TSA. Of the microRNAs significantly altered by HDACi treatment, 22 were up-regulated (Table II) and 10 were down-regulated (Table III). Their predicted (TargetScan and miRanda) or confirmed gene targets are provided.

Discussion

Drug resistance, acquired or *de novo*, remains a major obstacle in the treatment of cancer (1). Progression to resistance represents one of the hallmarks of aggressive carcinomas with limited treatment options and poor prognoses (2,3). Epigenetic therapies, including HDACi, provide a novel class of treatment for therapeutically-resistant cancer patients (32), including breast cancer (33). Here we demonstrate the ability of the HDACi TSA to suppress *in vitro* clonogenic survival of the apoptotically resistant MCF-7TN-R cells. This cell culture data indicates that in progressive drug resistance or recurrent breast carcinoma, the use of HDACis may exhibit greater inhibitory effects on tumor cell survival. Numerous studies have analyzed gene expression changes in response to HDACi, with the goal of defining specific mechanisms of their anticancer activity (34). Recent studies have also demonstrated the regulation of microRNA expression changes in breast and other cancer cells treated with HDACi alone (9,10,13,35), or in combination with DNMTi (11,36-38). Overall, these studies revealed microRNA expression profiles suggestive of a less aggressive and more tumor-suppressive phenotype after treatment with epigenetic therapies. Consistent with those studies, our microarray results revealed that many of the microRNAs that were significantly up-regulated (Table II) following TSA treatment (compared to control) have been characterized as having tumor suppressive

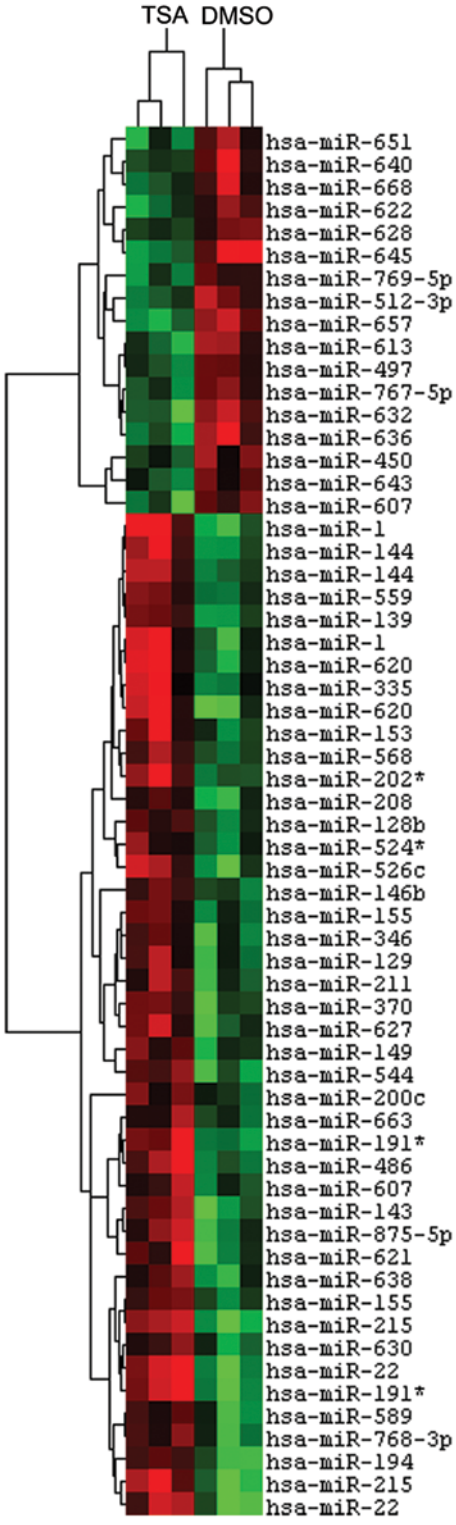

Figure 2. TSA regulation of microRNA expression in MCF-7TN-R. Heatmap of microRNA changes induced by treatment with TSA (10 μM) after 24 h in MCF-7TN-R cells. microRNAs demonstrating statistically significant changes in expression are shown (p<0.01). Green indicates down-regulated expression and red indicates up-regulated expression of microRNAs. Individual samples are represented in columns while specific microRNAs are represented by rows as labeled.

(miR-1, miR-143, miR-144, miR-191*, miR-202*, miR-486, miR-559), anti-migration/anti-metastasis (miR-22, miR-139, miR-194, miR-335), or anti-EMT (miR-215) roles in cancer.

Table II. Up-regulated miRNA following TSA treatment.

microRNA	Mean fold change	p-value	Description	Gene targets (ref.)
hsa-miR-1	2.44	<0.05	Tumor suppressor	cMET (39), TAGLN2 (40,41)
hsa-miR-22	2.69	<0.05	Anti-migration, cell cycle arrest	MYCBP, MAX
hsa-miR-139	1.61	<0.05	Anti-metastatic, tumor suppressor	ROCK2 (29), CDK6*, HOXB2*
hsa-miR-143	1.94	<0.05	Tumor suppressor	KRAS (42), BCL2 (43)
hsa-miR-144	1.97	<0.05	Tumor suppressor	Notch1 (44)
hsa-miR-153	1.70	<0.05	Tumor suppressor	BCL2 (45)
hsa-miR-155	1.53	<0.01	OncomiR	FOXO3A (46), SOCS1 (47), FADD and IKKE (48)
hsa-miR-191*	2.51	<0.05	Tumor suppressor	SPEN*
hsa-miR-194	1.70	<0.01	Tumor suppressor, anti-metastatic	CDH2, HBEGF, RAC1 and IGF1R (49)
hsa-miR-215	2.26	<0.01	Anti-EMT, cell cycle arrest	ZEB1/2 (50)
hsa-miR-202*	1.82	<0.05	Tumor suppressor	TGFBR2*, ROCK1*
hsa-miR-335	1.83	<0.05	Tumor suppressor, cell cycle arrest, metastasis suppressor	RB1/p105 (51), SOX4 and TNC (28)
hsa-miR-486	1.97	<0.05	Tumor suppressor	CD40 (52)
hsa-miR-526c	2.14	<0.05		
hsa-miR-544	1.74	<0.01		
hsa-miR-559	1.61	<0.05	Tumor suppressor	ERBB2 (53)
hsa-miR-568	1.59	<0.05		
hsa-miR-620	2.31	<0.05		
hsa-miR-627	1.93	<0.05		
hsa-miR-638	1.55	<0.01		
hsa-miR-641	2.02	<0.05		
hsa-miR-888	1.76	<0.05		

*Putative targets as indicated by TargetScan and miRanda.

Table III. Down-regulated miRNA following TSA treatment.

microRNA	Mean fold change	p-value	Description (ref.)	Gene targets (ref.)
hsa-miR-500	-1.90	<0.05	OncomiR (54)	
hsa-miR-512-3p	-1.59	<0.05		cFLIP (55)
hsa-miR-607	-1.68	<0.05		
hsa-miR-613	-1.69	<0.05		LXR (56)
hsa-miR-622	-1.57	<0.05		
hsa-miR-632	-1.86	<0.01		
hsa-miR-636	-2.00	<0.05		
hsa-miR-645	-2.03	<0.01	OncomiR (57)	
hsa-miR-651	-1.60	<0.05		
hsa-miR-657	-1.91	<0.01		IGF2R (58)

Only one known oncomiR, miR-155, was found to be increased following TSA treatment, but with a mean fold change of 1.53 compared to control, this was the lowest change observed, although statistically significant. Of the microRNAs identified as significantly decreased (Table III) following TSA treatment (compared to control), two have been identified as oncomiRs (miR-500, miR-645) and three others have confirmed targets involved in tumorigenesis (miR-512-3p, miR-613, miR-657). Taken together, these data indicate that HDACi treatment may promote an anti-tumor microRNA expression profile in the apoptotically resistant cell line MCF-7TN-R, providing novel therapeutic targets for the treatment of drug resistant breast cancer.

Acknowledgements

This research was supported by The Department of Defense Breast Cancer Research Program BC085426 (B.M. Collins-Burow); The National Institutes of Health/National Center for Research Resources P20RR020152 (B.M. Collins-Burow); The Integrated Cancer Biology Program: Centers for Cancer Systems Biology NIH/NCI U54CA113001 (K. Nephew); and The Walther Cancer Foundation, Indianapolis, IN (S.Y. Nam). The funders did not have any involvement in study design; the collection, analysis, or interpretation of the data; the writing of the manuscript; or the decision to submit the manuscript for publication.

References

1. Clarke R, Liu MC, Bouker KB, *et al*: Antiestrogen resistance in breast cancer and the role of estrogen receptor signaling. Oncogene 22: 7316-7339, 2003.
2. Garcia M, Derocq D, Freiss G and Rochefort H: Activation of estrogen receptor transfected into a receptor-negative breast cancer cell line decreases the metastatic and invasive potential of the cells. Proc Natl Acad Sci USA 89: 11538-11542, 1992.
3. van Agthoven T, Sieuwerts AM, Meijer-van Gelder ME, *et al*: Relevance of breast cancer antiestrogen resistance genes in human breast cancer progression and tamoxifen resistance. J Clin Oncol 27: 542-549, 2009.
4. Ting AH, McGarvey KM and Baylin SB: The cancer epigenome--components and functional correlates. Genes Dev 20: 3215-3231, 2006.
5. Lo PK and Sukumar S: Epigenomics and breast cancer. Pharmacogenomics 9: 1879-1902, 2008.
6. Sabnis GJ, Goloubeva O, Chumsri S, Nguyen N, Sukumar S and Brodie AM: Functional activation of the estrogen receptor-alpha and aromatase by the HDAC inhibitor entinostat sensitizes ER-negative tumors to letrozole. Cancer Res 71: 1893-1903, 2011.
7. Boumber Y and Issa JP: Epigenetics in cancer: what's the future? Oncology (Williston Park) 25: 220-226, 228, 2011.
8. Wilkes G: Histone deacetylase inhibitors. Oncology (Williston Park) 21: 39-40, 2007.
9. Zhang S, Cai X, Huang F, Zhong W and Yu Z: Effect of trichostatin a on viability and microRNA expression in human pancreatic cancer cell line BxPC-3. Exp Oncol 30: 265-268, 2008.
10. Shin S, Lee EM, Cha HJ, *et al*: MicroRNAs that respond to histone deacetylase inhibitor SAHA and p53 in HCT116 human colon carcinoma cells. Int J Oncol 35: 1343-1352, 2009.
11. Bandres E, Agirre X, Bitarte N, *et al*: Epigenetic regulation of microRNA expression in colorectal cancer. Int J Cancer 125: 2737-2743, 2009.
12. Saito Y, Suzuki H, Tsugawa H, *et al*: Chromatin remodeling at Alu repeats by epigenetic treatment activates silenced microRNA-512-5p with downregulation of Mcl-1 in human gastric cancer cells. Oncogene 28: 2738-2744, 2009.
13. Scott GK, Mattie MD, Berger CE, Benz SC and Benz CC: Rapid alteration of microRNA levels by histone deacetylase inhibition. Cancer Res 66: 1277-1281, 2006.
14. Ambros V: microRNAs: tiny regulators with great potential. Cell 107: 823-826, 2001.
15. Shenouda SK and Alahari SK: MicroRNA function in cancer: oncogene or a tumor suppressor? Cancer Metastasis Rev 28: 369-378, 2009.
16. Weldon CB, Parker AP, Patten D, *et al*: Sensitization of apoptotically-resistant breast carcinoma cells to TNF and TRAIL by inhibition of p38 mitogen-activated protein kinase signaling. Int J Oncol 24: 1473-1480, 2004.
17. Zhou C, Nitschke AM, Xiong W, *et al*: Proteomic analysis of tumor necrosis factor-alpha resistant human breast cancer cells reveals a MEK5/Erk5-mediated epithelial-mesenchymal transition phenotype. Breast Cancer Res 10: R105, 2008.
18. Xin F, Li M, Balch C, *et al*: Computational analysis of microRNA profiles and their target genes suggests significant involvement in breast cancer antiestrogen resistance. Bioinformatics 25: 430-434, 2009.
19. Thomson JM, Parker J, Perou CM and Hammond SM: A custom microarray platform for analysis of microRNA gene expression. Nat Methods 1: 47-53, 2004.
20. Eisen MB, Spellman PT, Brown PO and Botstein D: Cluster analysis and display of genome-wide expression patterns. Proc Natl Acad Sci USA 95: 14863-14868, 1998.
21. Di Leva G, Gasparini P, Piovan C, *et al*: MicroRNA cluster 221-222 and estrogen receptor alpha interactions in breast cancer. J Natl Cancer Inst 102: 706-721, 2010.
22. Antoon JW, Liu J, Gestaut MM, Burow ME, Beckman BS and Foroozesh M: Design, synthesis, and biological activity of a family of novel ceramide analogues in chemoresistant breast cancer cells. J Med Chem 52: 5748-5752, 2009.
23. Meacham WD, Antoon JW, Burow ME, Struckhoff AP and Beckman BS: Sphingolipids as determinants of apoptosis and chemoresistance in the MCF-7 cell model system. Exp Biol Med (Maywood) 234: 1253-1263, 2009.
24. Foekens JA, Sieuwerts AM, Smid M, *et al*: Four miRNAs associated with aggressiveness of lymph node-negative, estrogen receptor-positive human breast cancer. Proc Natl Acad Sci USA 105: 13021-13026, 2008.
25. Iorio MV, Ferracin M, Liu CG, *et al*: MicroRNA gene expression deregulation in human breast cancer. Cancer Res 65: 7065-7070, 2005.
26. Rao X, Di Leva G, Li M, *et al*: MicroRNA-221/222 confers breast cancer fulvestrant resistance by regulating multiple signaling pathways. Oncogene 30: 1082-1097, 2010.
27. Nana-Sinkam SP and Croce CM: MicroRNAs as therapeutic targets in cancer. Transl Res 157: 216-225, 2011.
28. Tavazoie SF, Alarcon C, Oskarsson T, *et al*: Endogenous human microRNAs that suppress breast cancer metastasis. Nature 451: 147-152, 2008.
29. Wong CC, Wong CM, Tung EK, *et al*: The microRNA miR-139 suppresses metastasis and progression of hepatocellular carcinoma by down-regulating Rho-kinase 2. Gastroenterology 140: 322-331, 2011.
30. Ma L, Teruya-Feldstein J and Weinberg RA: Tumour invasion and metastasis initiated by microRNA-10b in breast cancer. Nature 449: 682-688, 2007.
31. Ma L and Weinberg RA: MicroRNAs in malignant progression. Cell Cycle 7: 570-572, 2008.
32. Atadja PW: HDAC inhibitors and cancer therapy. Prog Drug Res 67: 175-195, 2011.
33. Munster PN, Thurn KT, Thomas S, *et al*: A phase II study of the histone deacetylase inhibitor vorinostat combined with tamoxifen for the treatment of patients with hormone therapy-resistant breast cancer. Br J Cancer 104: 1828-1835, 2011.
34. Shankar S and Srivastava RK: Histone deacetylase inhibitors: mechanisms and clinical significance in cancer: HDAC inhibitor-induced apoptosis. Adv Exp Med Biol 615: 261-298, 2008.
35. Lee EM, Shin S, Cha HJ, *et al*: Suberoylanilide hydroxamic acid (SAHA) changes microRNA expression profiles in A549 human non-small cell lung cancer cells. Int J Mol Med 24: 45-50, 2009.
36. Saito Y and Jones PA: Epigenetic activation of tumor suppressor microRNAs in human cancer cells. Cell Cycle 5: 2220-2222, 2006.
37. Saito Y, Liang G, Egger G, *et al*: Specific activation of microRNA-127 with downregulation of the proto-oncogene BCL6 by chromatin-modifying drugs in human cancer cells. Cancer Cell 9: 435-443, 2006.
38. Lujambio A and Esteller M: CpG island hypermethylation of tumor suppressor microRNAs in human cancer. Cell Cycle 6: 1455-1459, 2007.
39. Yan D, Dong Xda E, Chen X, *et al*: MicroRNA-1/206 targets c-Met and inhibits rhabdomyosarcoma development. J Biol Chem 284: 29596-29604, 2009.
40. Nohata N, Sone Y, Hanazawa T, *et al*: miR-1 as a tumor suppressive microRNA targeting TAGLN2 in head and neck squamous cell carcinoma. Oncotarget 2: 29-42, 2011.
41. Yoshino H, Chiyomaru T, Enokida H, *et al*: The tumour-suppressive function of miR-1 and miR-133a targeting TAGLN2 in bladder cancer. Br J Cancer 104: 808-818, 2011.
42. Xu B, Niu X, Zhang X, *et al*: miR-143 decreases prostate cancer cells proliferation and migration and enhances their sensitivity to docetaxel through suppression of KRAS. Mol Cell Biochem 350: 207-213, 2011.
43. Zhang H, Cai X, Wang Y, Tang H, Tong D and Ji F: microRNA-143, down-regulated in osteosarcoma, promotes apoptosis and suppresses tumorigenicity by targeting Bcl-2. Oncol Rep 24: 1363-1369, 2010.

44. Sureban SM, May R, Lightfoot S, *et al*: DCAMKL-1 regulates epithelial-mesenchymal transition in human pancreatic cells through a miR-200a-dependent mechanism. Cancer Res 71: 2328-2338, 2011.
45. Xu J, Liao X and Wong C: Downregulation of B-cell lymphoma 2 and myeloid cell leukemia sequence 1 by microRNA 153 induce apoptosis in a glioblastoma cell line DBTRG-05MG. Int J Cancer 126: 1029-1035, 2010.
46. Kong W, He L, Coppola M, *et al*: MicroRNA-155 regulates cell survival, growth, and chemosensitivity by targeting FOXO3a in breast cancer. J Biol Chem 285: 17869-17879, 2010.
47. Jiang S, Zhang HW, Lu MH, *et al*: MicroRNA-155 functions as an OncomiR in breast cancer by targeting the suppressor of cytokine signaling 1 gene. Cancer Res 70: 3119-3127, 2010.
48. Tili E, Michaille JJ, Cimino A, *et al*: Modulation of miR-155 and miR-125b levels following lipopolysaccharide/TNF-alpha stimulation and their possible roles in regulating the response to endotoxin shock. J Immunol 179: 5082-5089, 2007.
49. Meng Z, Fu X, Chen X, *et al*: miR-194 is a marker of hepatic epithelial cells and suppresses metastasis of liver cancer cells in mice. Hepatology 52: 2148-2157, 2010.
50. Kato M, Zhang J, Wang M, *et al*: MicroRNA-192 in diabetic kidney glomeruli and its function in TGF-beta-induced collagen expression via inhibition of E-box repressors. Proc Natl Acad Sci USA 104: 3432-3437, 2007.
51. Scarola M, Schoeftner S, Schneider C and Benetti R: miR-335 directly targets Rb1 (pRb/p105) in a proximal connection to p53-dependent stress response. Cancer Res 70: 6925-6933, 2010.
52. Mees ST, Mardin WA, Sielker S, *et al*: Involvement of CD40 targeting miR-224 and miR-486 on the progression of pancreatic ductal adenocarcinomas. Ann Surg Oncol 16: 2339-2350, 2009.
53. Chen H, Sun JG, Cao XW, *et al*: Preliminary validation of ERBB2 expression regulated by miR-548d-3p and miR-559. Biochem Biophys Res Commun 385: 596-600, 2009.
54. Yamamoto Y, Kosaka N, Tanaka M, *et al*: MicroRNA-500 as a potential diagnostic marker for hepatocellular carcinoma. Biomarkers 14: 529-538, 2009.
55. Chen F, Zhu HH, Zhou LF, Wu SS, Wang J and Chen Z: Inhibition of c-FLIP expression by miR-512-3p contributes to taxol-induced apoptosis in hepatocellular carcinoma cells. Oncol Rep 23: 1457-1462, 2010.
56. Ou Z, Wada T, Gramignoli R, *et al*: MicroRNA hsa-miR-613 targets the human LXR(alpha) gene and mediates a feedback loop of LXR(alpha) autoregulation. Mol Endocrinol 25: 584-596, 2011.
57. Shih KK, Qin LX, Tanner EJ, *et al*: A microRNA survival signature (MiSS) for advanced ovarian cancer. Gynecol Oncol 121: 444-450, 2011.
58. Lv K, Guo Y, Zhang Y, Wang K, Jia Y and Sun S: Allele-specific targeting of hsa-miR-657 to human IGF2R creates a potential mechanism underlying the association of ACAA-insertion/deletion polymorphism with type 2 diabetes. Biochem Biophys Res Commun 374: 101-105, 2008.

Targeting triple-negative breast cancer cells with the HDAC inhibitor Panobinostat

[#]Chandra R. Tate, [#]Lyndsay V. Rhodes, H. Chris Segar, Jennifer L. Driver, F. Nell Pounder, Matthew E. Burow, and Bridgette M. Collins-Burow[*]

Department of Medicine, Section of Hematology and Medical Oncology, Tulane University Health Sciences Center, New Orleans, LA.

Email addresses

CRT: ctate@tulane.edu

LVR: lvanhoy@tulane.edu

HCS: hsegar@tulane.edu

JLD: jdriver@tulane.edu

FNP: fkeith@tulane.edu

MEB: mburow@tulane.edu

BMC: bcollin1@tulane.edu

Corresponding Author *

Bridgette M. Collins-Burow, 1430 Tulane Ave, SL-78, New Orleans, LA 70112. Phone: 504-988-6879; Fax: 504-988-5483; Email: bcollin1@tulane.edu

[#] Denotes authors contributed equally to this work.

Abstract

Introduction: Of the more than one million global cases of breast cancer diagnosed each year, approximately fifteen percent are characterized as triple-negative, lacking the estrogen, progesterone, and Her2/neu receptors. Lack of effective therapies, younger age at onset, and early metastatic spread have contributed to the poor prognoses and outcomes associated with these malignancies. Here, we investigate the ability of the histone deacetylase inhibitor Panobinostat (LBH589) to selectively target triple-negative breast cancer (TNBC) cell proliferation and survival *in vitro* and tumorigenesis *in vivo*.

Methods: TNBC cell lines MDA-MB-157, MDA-MB-231, MDA-MB-468, and BT-549 were treated with nanomolar (nM) quantities of LBH589. Relevant histone acetylation was verified by flow cytometry and immunofluorescent imaging. Assays for trypan blue viability, MTT proliferation, and DNA fragmentation were used to evaluate overall cellular toxicity. Changes in cell cycle progression were assessed with propidium iodide flow cytometry. Additionally, qPCR arrays were used to probe MDA-MB-231 cells for LBH589-induced changes in cancer biomarkers and signaling pathways. Orthotopic MDA-MB-231 and BT-549 mouse xenograft models were used to assess the effects of LBH589 on tumorigenesis. Lastly, flow cytometry, ELISA, and immunohistochemical staining were applied to detect changes in CDH1 protein expression and the results paired with confocal microscopy in order to examine changes in cell morphology.

Results: LBH589 treatment increased histone acetylation, decreased cell proliferation and survival, and blocked cell cycle progression at G2/M with a concurrent decrease in S phase in all TNBC cell lines. Treatment also resulted in apoptosis induction at 24 hours in all lines except the MDA-MB-468 cell line. MDA-MB-231 and BT-549 tumor formation was significantly

inhibited by LBH589 (10 mg/kg/day) in mice. Additionally, LBH589 up-regulated CDH1 protein *in vitro* and *in vivo* and induced cell morphology changes in MDA-MB-231 cells consistent with reversal of the mesenchymal phenotype.

Conclusions: This study revealed that LBH589 is overtly toxic to TNBC cells *in vitro* and decreases tumorigenesis *in vivo*. Additionally, treatment up-regulated anti-proliferative, tumor suppressor, and epithelial marker genes in MDA-MB-231 cells and initiated a partial reversal of the epithelial-to-mesenchymal transition. Our results demonstrate a potential therapeutic role of LBH589 in targeting aggressive triple-negative breast cancer cell types.

Keywords: Panobinostat, LBH589, triple-negative breast cancer, xenograft, histone deacetylase inhibitor, E-cadherin, CDH1, epithelial-to-mesenchymal transition

Introduction

Over 200,000 new cases of invasive breast cancer are diagnosed in the United States each year and approximately 40,000 of the patients diagnosed will die from the disease [1]. Breast cancers are routinely classified by stage, pathology, grade and expression of estrogen receptor (ER), progesterone receptor (PR) or human epidermal growth factor receptor (Her2/neu). Current successful therapies include hormone-based agents that directly target these receptors [2, 3]. Triple-negative breast cancer (TNBC) is a heterogeneous subset of neoplasms that is defined by the absence of these targets [4-6]. Approximately 15% of globally diagnosed breast cancers are designated as ER-, PR- and Her2/neu-negative [1, 7, 8]. Studies have shown that tumors of this aggressive subtype are of higher histological grade, affect a disproportionate number of young women, and are more likely to recur earlier at distant sites, resulting in poor overall prognoses [4, 5, 9, 10]. To improve outcomes of TNBC, we must unravel its biological pathways and modes of progression and use that knowledge to develop novel targets and therapies.

Histone deacetylase inhibitors (HDACis) have emerged as a promising new class of multifunctional anticancer agents [11, 12]. That promise lies in the ability of HDACis to effect multiple epigenetic changes in aberrant cells. In addition to regulating gene expression and transcription through chromatin remodeling, HDACis can also modulate a variety of cellular functions including growth, differentiation, and survival [13, 14] due, in part, to their ability to enhance acetylation of a wide range of proteins, including transcription factors, molecular chaperones, and structural components [11, 15, 16]. Specifically, HDACis have been linked to several downstream effects in tumor cell lines which include: cell cycle arrest, induction of apoptosis, inhibition of angiogenesis, activation or inactivation of tumor suppressor genes or oncogenes, and decreased invasion and metastases [11, 12, 17].

Panobinostat (LBH589) is a potent pan-deacetylase inhibitor that can block multiple cancer related pathways and reverse epigenetic events implicated in cancer progression [18]. HDACs can be subdivided into two groups: zinc-dependent (Class I, II, and IV) and zinc-independent (Class III) [19]. Panobinostat (LBH589) is a potent inhibitor with activity against Class I, II, and IV HDAC enzymes, suggesting true pan-HDAC activity [18]. In preclinical studies, LBH589 has shown potent inhibitory activity at low nanomolar concentrations across a wide range of hematologic malignancies including lymphoma, multiple myeloma and acute myeloid leukemia [20-22]. It is also being investigated as treatment against non-responsive solid tumors as well as tumors of lung, thyroid, and prostate [23-26]. It has shown synergy with chemotherapeutics, radiation, demethylators, proteasome inhibitors, and other agents [27-29]. Based on these preclinical findings, LBH589 and other HDACis have undergone a rapid phase of clinical development with many entering clinical trials, both as single agents or in combination with other therapies [12, 23, 30, 31]. To date, LBH589 has demonstrated favorable clinical responses, with limited toxicity [23, 32, 33]. There is a critical need to develop pleiotropic therapies that specifically target the neoplasm as well as the biological pathways and markers of TNBC progression. The purpose of this study was to determine the ability of LBH589 to selectively target the TNBC subtype of breast cancer cells, assessed by the effects on the growth, survival, and tumorigenesis of a representative panel of TNBC cells. We also sought to characterize the effects LBH589 on the regulation of breast cancer genes, related signaling pathways and morphology.

Materials and Methods

Cell lines and reagents

Human TNBC (MDA-MB-157, MDA-MB-231, MDA-MB-468, BT-549), MDA-MB-361 and HEK293T (human embryonic kidney) cell lines and were obtained from the American Type Culture Collection (ATCC, Manassas, VA). MDA-MB-157, MDA-MB-231, and BT-549 cells are characterized as triple-negative/basal-B mammary carcinoma, while the MDA-MB-468 cells are characterized as triple-negative/basal-A mammary carcinoma. MDA-MB-361 cells are characterized as ER-positive/PgR-negative, luminal mammary carcinoma. Liquid nitrogen stocks were made upon receipt and maintained until the start of each study. MCF-7 cells, characterized as ER-positive/PgR-positive luminal mammary carcinoma, were obtained from frozen stocks routinely used in previous experiments [34]. The ER-positive/PgR-positive ZR-75-1 human epithelial mammary ductal carcinoma cells were a generous gift of Dr. Brian Rowan (Tulane University, New Orleans, LA). Cells were used for no more than 6 months after being thawed with periodic recording of morphology and doubling times to ensure maintenance of phenotype. Cells were maintained at 37^{o}, 5% CO_2 in Dulbecco's modified Eagle's medium (10% DMEM; Invitrogen, Carlsbad, CA) supplemented with 10% fetal bovine serum (Hyclone, Salt Lake City, UT) and 1% penicillin/streptomycin (Invitrogen, Carlsbad, CA). LBH589 was generously provided by Novartis Pharmaceutical Inc. (East Hanover, NJ). LBH589 was dissolved in dimethyl sulfoxide (DMSO) (Invitrogen, Carlsbad, CA) as a 1 mM stock solution and kept at -20 °C. The drug was diluted in culture media and used at various concentrations as indicated.

Histone acetylation

TNBC cells were plated at 70% confluency in 10% DMEM and allowed to attach overnight. Cells were treated with LBH589 (100nM, 200nM) or vehicle for 18 hours, then fixed, permeabilized and stained with acetyl-histone H3 (Lys9) antibody /Alexa Fluor® 488 Conjugate or acetyl-histone H4 (Lys8) antibody/ Alexa Fluor® 488 Conjugate (Cell Signaling Technology, Danvers, MA), followed by rhodamine phalloidin, and DAPI (4′,6-diamidino-2-phenylindole) counterstain (Molecular Probes, Carlsbad, CA) per manufacturer's instructions. Cells were dually analyzed by BD LSR II flow cytometer and BD Pathway 855 bioimaging confocal system and images merged using BD Attovision™ Software (BD Biosciences, San Jose, CA). Data is represented as mean fluorescence intensity (mean ± SEM) of two independent experiments with internal triplicates.

MTT Cell Proliferation Assay

Proliferation was measured by MTT (3-(4, 5-dimethylthiazol-2-yl)-2,5-diphenyltetrazolium bromide) Cell Proliferation Assay, according to the manufacturer's protocol (ATCC, Manassas, VA). Briefly, cells were plated in 96-well flat bottom plates at a density of $5x10^3$ per 100µl in 10% DMEM, allowed to attach overnight, and then treated with LBH589 (50, 100, 200 nM) or vehicle for 24 hours. MTT reagent (10µl) was added to each well (final concentration 0.5 mg/ml) and the plate incubated at 37°C. After 4 hours, 100µl of solubilization solution (10% SDS) was added to each well and the plate incubated for 2 hours. A matched control cell standard curve using sequentially increased cell numbers was included on the plate for each corresponding cell line to determine growth inhibition. The absorbance was read at 570nm on a *Synergy*™ 4 Multi-Mode Microplate Reader and analyzed with Gen5™ Data Analysis Software (*BioTek,* Winooski, VT). Data represented as mean percent vehicle treated cell proliferation ± SEM of triplicate experiments with internal triplicates.

Trypan blue viability assay

Cells were plated in 96-well plates at a density of $5x10^3$ per 100µl in 10% DMEM and allowed to adhere overnight. Cells were treated with vehicle or LBH589 (50, 100, 200 nM) for 24 hours and harvested by trypsinization. Cells were then stained with a trypan blue solution (0.04% w/v, Invitrogen, Carlsbad, CA), and counted on a Cellometer Vision automated cell counter (Nexcelom Bioscience, Lawrence, MA) per the manufacturer's protocol. Cell viabilities are represented as mean percent relative to matched, vehicle-treated cells ± SEM of triplicate experiments with internal triplicates.

Apoptosis

Analysis of apoptosis was carried out using the Cell Death Detection ELISA^{PLUS} according to the manufacture's protocol (Roche Applied Science, Germany). This quantitative DNA fragmentation immunoassay uses monoclonal antibodies directed against histone-complexed DNA. Briefly, cells (10^4 cells/well) were plated in 96 well plates overnight and treated for 24 hours with LBH589 (100, 200 nM) or vehicle control. After cell lysis and centrifugation, the cell lysates were tested for histone-complexed DNA fragments. The absorbance was read at 405 nm on a Synergy™ HT Multi-Mode Microplate Reader and analyzed with Gen5™ Data Analysis Software (Bio-Tek, Winooski, VT). Apoptosis of the treated cells was expressed as mean enrichment factor (treated cells over vehicle controls) ± SEM of duplicate experiments with internal triplicates.

Cell cycle analysis

For cell cycle analysis, TNBC cells were plated overnight in 10% DMEM and treated with 100nM LBH589 for 24 or 72 hours. Both floating cells and trypsinized adherent cells were

collected and combined for analysis. Cells were fixed by dropwise addition into ice cold ethanol and stored at -20^{o} overnight. Cells were then pelleted, washed, and stained for one hour with 50 μg/ml propidium iodide in PBS containing 0.1mg/ml ribonuclease A and 0.05% Triton X-100 (Sigma, St. Louis, MO). After gating to exclude debris, the DNA content was measured using a LSR-II flow cytometer (BD Biosciences, San Jose, CA). Data was analyzed with ModFit LT software (Verity Software House, Topsham, ME). Data represented as percent live cells of two independent experiments.

Plasmid packaging and stable cell line generation

HEK293T cells were plated at 5.5 x 10^6 in a 10 cm dish in 10ml of 10% DMEM and allowed to adhere overnight. The following day, the HEK293t cells were co-transfected with the pLEmiR non-silencing turbo red fluorescent protein (tRFP) vector construct (9μg) and the trans-lentiviral packaging mix and pLEX^{TM} transfer vector using the TransLenti Viral pLEX packaging system, following the manufacturer's instructions (Thermo Scientific, Waltham, MA). Virus was harvested 48 hours post-transfection and stored at -80^{o}C. TNBC cell lines were plated at 70% confluence in 10 cm dishes with 10ml of 10% DMEM and allowed to adhere overnight. The following day, cells were transduced with virus containing the pLEmiR tRFP vector (1:10 dilution) in serum-free media following manufacturer's protocol. After 4 hours, the transduction media was removed and replaced with 10% DMEM. After 24 hours, cells were treated with puromycin (Invitrogen, Carlsbad, CA) to select for vector expression. The resultant stable transfectants were designated as MDA-MB-231-tRFP and BT-549-tRFP.

Animal xenograft studies

Xenograft tumor studies were conducted as previously described [34]. In short, CB-17/SCID female mice (4-6 weeks old) were obtained from Charles River Laboratories (Wilmington, MA). The animals were allowed a period of adaptation in a sterile and pathogen-free environment with food and water *ad libitum*. MDA-MB-231-tRFP and BT-549-tRFP cells were harvested in the exponential growth phase using a PBS/EDTA solution and washed. Viable cells (5×10^6) in 50 µl of sterile PBS suspension were mixed with 100µl reduced growth factor Matrigel (BD Biosciences, Bedford, MA) and injected bilaterally into the inguinal mammary fat pad. On day three post cell injection, mice were randomized into treatment groups of five mice each: (vehicle control or 10 mg/kg LBH589). Beginning on day 14 post cell injection, animals received intraperitoneal (i.p.) injections of the corresponding drug treatment on a 5-day on and 2-day off schedule for 28 days [18]. Tumor size was measured with a digital caliper and calculated using the formula $4/3\pi LS^2$ (L=larger radius, S=smaller radius). At necropsy, animals were euthanized by cervical dislocation following CO_2 exposure. Tumors, livers, lungs, and brains were removed and snap frozen or fixed in 10% formalin for future analysis. All procedures involving animals were conducted in compliance with State and Federal laws, the U.S. Department of Health and Human Services, and guidelines established by Tulane University Animal Care and Use Committee. The facilities and laboratory animals program of Tulane University are accredited by the Association for the Assessment and Accreditation of Laboratory Animal Care.

Human breast cancer quantitative reverse transcription real-time PCR array

Human Breast Cancer and Estrogen Receptor Signaling RT² Profiler™ PCR Arrays (PAHS-005) were obtained from SABiosciences (Frederick, MD). MDA-MB-231, MCF-7, and MDA-MB-468 cells were plated in 10% DMEM at 70% confluency and treated with 100nM LBH589 or vehicle for 24 hours. Cells were harvested by trypsinization and total RNA was isolated using the

RNeasy kit, per manufacturer's instructions (Qiagen, Valencia, CA). The quantity and quality of the RNA were determined by absorbance at 260 and 280 nm using the NanoDrop ND-1000 (NanoDrop, Wilmington, DE). Total RNA (1.5 µg) was reverse-transcribed using the RT^2 First Strand cDNA synthesis kit, following the manufacturer's protocol (SABiosciences, Frederick, MD) and then assayed via an optimized, quantitative reverse transcription real-time PCR (qPCR) array to assess LBH589-associated changes in the expression of 84 genes related to breast cancer regulation and estrogen receptor-dependent signal transduction, according to the manufacturer's protocol. Biological triplicates were run for each sample.

CDH1 flow cytometry and immunofluorescent imaging

MDA-MB-231 cells were plated at 70% confluency in 10% DMEM and allowed to attach overnight. Cells were then treated with LBH589 (100 nM) or vehicle for 24 hours. Cells were harvested by gentle pipetting (PBS with 5% FBS), fixed, and stained with Alexa Fluor® 488-conjugated CDH1 (E-cadherin) antibody (BD Biosciences, San Jose, CA). The expression of CDH1 protein was determined by flow cytometry on a BD LSRII instrument. Data represented as mean percent E-cadherin positive cells ± SEM of duplicate experiments with internal triplicates. Paired cells were seeded on BD Falcon 96-well black imaging plates. Staining is represented by the following colors: Green = CDH1, Red = phaloidin, Blue = DAPI nuclear stain. Confocal immunofluorescent images were captured on the BD Pathway 855 Bioimaging system and merged using BD Attovision™ software (BD Biosciences, San Jose, CA).

ELISA for CDH1

MDA-MB-231 cells (10^5 cells/well) were plated overnight in 6-well plates and then treated for 24 hours with LBH589 (100 nM) or vehicle control. Five volumes of ice-cold lysis buffer (20

mM Tris-HCl, pH 7.5/150mM NaCl/1 mM EDTA/1 mM EGTA/1% Tween 20) supplemented with protease inhibitor tablets (Roche Diagnostics, Indianapolis, IN) was added to each well. Cell lysates were mechanically dissociated and centrifuged (10,000 × *g* for 15 minutes at 4°C), and then diluted 1:1 with calibrator diluent. CDH1 levels were then determined by human CDH1 ELISA per the manufacturer's instructions (R&D Systems, Minneapolis, MN). The absorbance was read at 450 nm on a Synergy™ HT Multi-Mode Microplate Reader (Bio-Tek, Winooski, VT). Data represented as mean pg/ml of CDH1 ± SEM of duplicate experiments with internal triplicates.

Immunohistochemical staining

Representative sections of tumor with adjacent tissues were fixed in 10% neutral buffered formalin for 24 to 36 hours. Paraffin-embedded sections were prepared at 4 μm thickness followed by standard hematoxylin and eosin (H&E) staining. Additional sections were manually deparaffinized in xylene, rehydrated in a series of graded ethanol solutions, boiled in10mM sodium citrate buffer (pH 6.0) for 10 minutes, then cooled for 20 minutes for antigen retrieval. Sections were blocked for 30 minutes with 10% normal goat serum (Invitrogen, Carlsbad, CA), incubated overnight in a 4^{o} humidified chamber with rabbit anti-E-cadherin (Abcam, UK) at 1:30 dilution, followed by 1 hour incubation with Alexa Fluor® 488 goat anti-rabbit secondary (Invitrogen, Carlsbad, CA). Fluorescent images were captured on a Nikon TE2000 inverted microscope with IPLab software (BD Biosciences, Rockville, MD).

Statistical analyses

Statistical analyses were carried out with GraphPad Prism software (Graph-Pad Software, Inc., San Diego, CA). Studies involving more than two groups were analyzed by one-way analysis of

variance (ANOVA) followed by Tukey's post-hoc multiple comparison tests. All others were subjected to unpaired Student's t-test, with $p<0.05$ considered statistically significant.

Results

LBH589 induces histone acetylation

To verify the effects of LBH589 as a relevant histone deacetylase inhibitor, four TNBC cell lines, MDA-MB157, MDA-MB-231, MDA-MB-468, and BT-549, were treated with increasing concentrations of the drug (100-200nM) and assayed after 18 hours by flow cytometry for antibodies to acetylated histones H3 and H4. As can be seen in Figures 1A-1B, LBH589 induced hyper-acetylation of histones H3 (Lys9) and H4 (Lys8) in all four tested TNBC cell lines, as seen in Figures 1A and 1B, respectively (***, $p < 0.001$). MDA-MB-468 cells were the least responsive to LBH589 with a 2.1-fold change compared to vehicle treated cells. Additionally, three color confocal immunofluorescence imaging was conducted to visually confirm the increased accumulation of acetylated histones H3 (Figure 1C) and H4 (Figure 1D) in the LBH589-treated cells.

LBH589 cytotoxicity in TNBC cell lines

To determine the effect of LBH589 on cell proliferation and survival *in vitro*, three ER-positive and four TNBC cell lines were treated with increasing doses (50, 100, 200 nM) of drug for 24 hours. LBH589 induced a significant dose-dependent decrease in proliferation in all four tested TNBC cell lines, as assayed by MTT metabolism (Figure 2A). At 200nM, all TNBC cells had greater than 40% reduction in proliferation compared to vehicle treated cells ($p < 0.001$). In contrast, growth of ER-positive cell lines (MCF-7, ZR-75-1, and MDA-MB-361) was not significantly affected by LBH589. In order to confirm the accuracy of the MTT assay, trypan

blue assays were also conducted as a measure of membrane integrity (Figure 2B). Again, cell viability was significantly decreased in the TNBC cell lines at all doses compared to vehicle controls, with a greater than 25% decrease in cell viability observed at 200nM in all TNBC cell lines ($p < 0.001$). As with the MTT assay, LBH589 treatment did not affect ER-positive cell viability as measured by trypan blue.

Effects of LBH589 on cell cycle progression were analyzed by propidium iodide flow cytometry at 24 and 72 hours. LBH589 (100nM) induced G2/M cell cycle arrest, as evidenced by accumulation of cells in G2/M, with concurrent decrease in S phase peaks in all four tested TNBC cell lines (Table 1). Treatment also induced a time-dependent increase in sub-G/debris fraction in all four TNBC cell lines (data not shown).

LBH589-induced apoptosis, as measured by DNA fragmentation, was assessed at 24 hours in the TNBC cell lines. A clear induction of apoptosis was apparent at 100nM and 200nM concentrations in three of the four tested TNBC cell lines ($p < 0.001$), with a mean increase of 304 ± 0.78% at 200nM (Figure 3A). Enrichment was not significant in the MDA-MB-468 cell line at this time point. Visual evidence of LBH589-induced apoptosis (arrows) is presented in the panel of confocal immunofluorescence images shown in Figures 3B.

LBH589 targets tumor growth *in vivo*

To determine if the anti-cancer effects of LBH589 observed *in vitro* translated to decreased tumorigenesis *in vivo,* immunocompromised female mice were orthotopically inoculated with MDA-MB-231 (Figure 4A) or BT-549 (Figure 4B) cells ($5x10^6$ cells/site, bilaterally) and treated with LBH589 or vehicle control. Treatment with LBH589 (10mg/kg/day, 5 days/week) resulted in significant decreases in tumor volume with 3- to 4-fold (BT549 and MDA-MB-231,

respectively) inhibition of tumor volumes compared to controls by day 41 (28 days post treatment, $p < 0.001$). There was no overt toxicity, as measured by weight loss, noted at this dose and treatment schedule.

LBH589 regulates breast cancer genes and estrogen signaling pathways.

To reveal possible molecular mechanisms and signaling pathways involved in TNBC cell response to LBH589, MDA-MB-231 cells were treated for 24 hours and analyzed with the Human Breast Cancer and Estrogen Receptor Signaling RT² Profiler™ PCR Array (SABiosciences Frederick, MD). As shown in Supplemental Table 1, thirty-five of the eighty-four representative genes were significantly altered at least 2-fold ($p<0.05$). Specifically, expression of twenty-four genes was up-regulated while expression of eleven genes was suppressed. Of particular interest was the 31-fold increase in the documented epithelial cell marker/tumor suppressor, CDH1 (E-cadherin) [35]. Also noted were decreases in the proliferation marker MKI67 and upregulation of the tight-junction protein, claudin-7.

To further investigate whether the above LBH589-induced changes were specific to the basal-B subtype, MDA-MB-468 (basal-A) and MCF-7 (luminal) cell lines were also tested by Human Breast Cancer and Estrogen Receptor Signaling RT² Profiler™ PCR Array following 24 hours of LBH589 treatment. The representative heat map illustrates the changes in gene expression of all three cell lines following LBH589 treatment as compared to MDA-MB-231 vehicle treated cells (Figure 5). Supplemental Table 2 shows the twenty-four significantly altered genes in the MDA-MB-468 cells following LBH589 treatment ($p<0.05$), with nineteen up-regulated and five genes down-regulated. Of the up-regulated genes, many are known to be involved in the promotion of cell proliferation, survival, and tumor progression (CCNA1, CCNE1, FOSL1, ITGB4, PAPPA, RAC2, SERPINB5), while only three tumor suppressive genes (CDKN1A, SPRR1B, THBS1)

were increased by LBH589 in the MDA-MB-468 cell system. Supplemental Table 3 shows the thirty-four genes significantly altered by LBH589 in MCF-7 cells ($p<0.05$). Of these altered genes, twenty-four were up-regulated while ten genes were down-regulated. Again, many of the up-regulated genes have known roles in cell proliferation, survival, and tumorigenesis (CCNA1, FGF1, ITGA6, KLF5, SERPINE1, SLC7A5) in the MCF-7 cells. Additionally, the well known metastasis suppressor NME1 was decreased by LBH589 in these cells. Overall, these array data reveal a profile consistent with a less aggressive, and more favorable prognostic profile for MDA-MB-231 cells treated with LHB589, while the less biologically sensitive MDA-MB-468 and MCF-7 cell lines display a less clear cut picture for LBH589-induced gene expression in cells of the basal-A and luminal subtypes. **LBH589 induces changes in morphology and CDH-1 expression of MDA-MB-231 cells consistent with reversal of EMT.**

To assess potential LBH589-induced changes in morphology and cytoskeletal protein expression in mesenchymal cells, MDA-MB-231 cells were treated with LBH589 (100 nM) for 24 hours and analyzed. Figure 6A shows a significant increase of CDH1-positive cells in LBH589 treated cells compared to control (48.5 ± 2.3 % to 9.70 ± 0.569 %, respectively; $p < 0.001$). In confirmation, cells were also assayed by ELISA, which showed a 1.6-fold increase in CDH1 protein levels over controls (Figure 6B, $p<0.001$). These results are consistent with our qPCR array finding of 31-fold up-regulation of CDH1 expression in MDA-MB-231cells (Table 2). MDA-MB-231 cells also exhibited partial reversal of the mesenchymal phenotype, as evidenced by a shift from spindle shaped cells with visible actin stress fibers to predominantly cuboidal/spherical forms with cortical actin patterns [36-38], following 24 hour treatment with LBH589 (Figures 6C). To determine if the *in vitro* up-regulation of CDH1 also occurred *in vivo*,

MDA-MB-231 primary tumor sections were stained for CDH1. As can be seen in Figure 7, there is increased CDH1 staining along the periphery of the LBH589 treated tumor.

Discussion

In recent years, an increasing number of HDACis have been identified, developed, and advanced to clinical trials [39-40]. LBH589 has shown potent activity at low nanomolar concentrations across a wide range of hematologic malignancies and solid tumors in preclinical studies [20-22, 41]. Others have demonstrated that HDACi treatment can suppress oncogenes and induce re-expression of previously silenced tumor suppressors and receptors such as the ER [24, 42-44]. In addition to its single agent effects, recent studies have demonstrated a role for LBH589 in resensitizing cancer cells to other agents including chemotherapy [45], radiation [46], autophagy inhibitors [47], and endocrine therapies including tamoxifen [48] and letrozole [49]. In consideration of the promising results reported by others, we endeavored to determine whether LBH589 would be effective against a panel of breast cancer cell lines that display common characteristics of the triple-negative subtype.

In this study, we utilized MDA-MB-157, MDA-MB-231, MDA-MB-468, and BT549 cell lines as models of TNBC growth and progression. In confirmation of other preclinical research [20, 24, 42, 44, 50, 51], we found that LBH589 induced hyperacetylation of histones H3 and H4, decreased proliferation and survival, and induced apoptosis and G2/M cell cycle arrest. The MDA-MB-231 and BT549 lines were chosen as models for our *in vivo* xenograft studies using CB-17/SCID mice. Treatment with LBH589 decreased MDA-MB-231 and BT549 tumor significantly with minimal animal toxicity, providing preclinical data on the effectiveness of LBH589 on TNBC tumorigenesis at a low and well tolerated dose.

The LBH589-induced effects on cell proliferation and survival appear to be TNBC cell specific as the ER-positive cell lines tested were unaffected at all doses tested (up to 200 nM), contrary to previously published work which reported LBH589 significantly inhibited cell survival and induced cell death in ER-positive and ER-negative breast cancer cell lines [44, 47]. We propose that the more aggressive, highly proliferative nature and invasive phenotype of TNBC cells render them particularly susceptible to the effects of LBH589. Of the four TNBC cell lines tested, the MDA-MB-468 cells were the most resistant to hyper-acetylation and DNA degradation by the drug. This is interesting as this cell line is the most phenotypically different (spherical morphology) and least invasive of the four tested cell lines. The MDA-MB-157, MDA-MB-231, and BT549 lines have been classified as basal-B [52], with the MDA-MB-231 and BT-549 cell lines specifically classified as mesenchymal (stellate), claudin-low, and highly invasive [53-56]. The MDA-MB-157 cells are classified as mesenchymal, claudin-low, and moderately invasive [52]. Clinically, the majority of claudin-low tumors are of the triple-negative subtype and are associated with poor overall prognoses [53]. However, MDA-MB-468 cells have been characterized under the basal-A subtype, as they possess both basal (triple-negative) and luminal (spherical morphology) characteristics and are only minimally invasive [52]. Additionally, super array data comparing LBH589-induced gene expression changes between LBH589-sensitive (MDA-MB-231, basal-B) and LBH589-insensitive (MDA-MB-468, basal-A; MCF-7, luminal) cells revealed several changes specific to the basal-B subtype (see bolded genes in Supplemental Table 1). These ten genes included known regulators cell proliferation (FOSL1, STC2, TGFA, THBS2) and apoptosis (FAS, FASLG), as well as angiogenesis (TNFAIP2). Additionally, many of the genes altered by LBH589 specifically in MDA-MB-231 cells have documented roles in cell invasion and metastasis including CDH1,

CLDN7, FOSL1, PLAU, STC2, and TGFA. These data support the role of the selective effects of LBH589 observed on the basal-B cell lines compared to the other subtypes tested. Interestingly, superarray data identified CDH1 as being the most induced gene by LBH589 treatment specifically in MDA-MB-231 cells, as these cells are characterized as mesenchymal, thus lacking significant CDH1 expression. The TNBC subtype is exemplified by its highly aggressive and metastatic nature. A known key step in the process of metastasis is the epithelial-to-mesenchymal transition (EMT). This oncogenic EMT is typified by increased invasion and metastatic dissemination, therapeutic resistance and loss of expression of tumor suppressors such as CDH1 [57, 58]. Studies have demonstrated that EMT and the resultant loss of CDH1 expression are crucial steps in tumor progression and correlate with poor clinical outcomes [59-61]. In confirmation of our *in vitro* data on CDH1 up-regulation, we also noted an increase in CDH1 on the periphery of the primary tumor from our MDA-MB-231 xenograft model. Decreased CDH1 expression at the tumor periphery has been linked to increased metastasis-risk and decreased overall patient survival [62]. Induction of CDH1 expression by LHB589 at the invasive edge may therefore be indicative of decreased metastatic potential. LBH589-induced re-expression of CDH1, along with other morphological features, indicates the partial reversal of EMT, a target of enormous potential particularly in the TNBC subtype. This suggests LBH589 as a promising therapeutic option for the more aggressive, TNBC/basal-like breast cancer subtypes.

Conclusions

Our results illustrate the ability of LBH589 to hyperacetylate histones, inhibit proliferation and survival, and decrease *in vivo* tumorigenesis of TNBC cells. Our *in vitro* data suggest that this cytotoxicity is partially due to cell cycle arrest and apoptosis. Also noted in treated cultures was an apparent partial reversal of the mesenchymal phenotype evidenced by increased CDH1

protein expression and morphology changes in MDA-MB-231 cells. This increased CDH1 was confirmed with measured upregulation of the CDH1 staining at the primary tumor periphery in our xenograft model. Overall, our results affirm the efficacy and demonstrate a potential therapeutic role of LBH589 in targeting aggressive triple-negative breast cancer cell types.

Abbreviations

BT-549-tRFP	BT-549 turbo red transfectant
CDH1	Cadherin-1, E-cadherin
DAPI	4′,6-diamidino-2-phenylindole.
10%DMEM	Dulbecco's modified Eagle's medium with 10% fetal bovine serum
DMSO	Dimethyl sulfoxide
ELISA	Enzyme-linked immunosorbent assay
EMT	Epithelial-to-mesenchymal transition
ER	Estrogen receptor
HDAC	Histone deacetylase
HDACi	Histone deacetylase inhibitor
H&E	Hematoxylin and eosin
Her2/neu	Human epidermal growth factor receptor 2
i.p.	Intraperitoneal
LBH589	Panobinostat
MDA-MB-231-tRFP	MDA-MB-231 turbo red transfectant
MT3	Metallothionein 3
MTT	3-(4,5-dimethylthiazol-2-yl)-2,5-diphenyltetrazolium bromide
nM	Nanomolar
PR	Progesterone receptor
qPCR	Quantitative reverse transcription real-time polymerase chain reaction
SCID	Severe combined immunodeficiency
TNBC	Triple-negative breast cancer

tRFP	Turbo red fluorescent protein

Competing interests

The authors declare no competing interests.

Authors' Contributions

CRT drafted the manuscript and conducted histone acetylation, proliferation, viability, apoptosis, cell cycle, flow cytometry, ELISA, and BD pathway analyses, as well as xenograft studies and statistical analyses. LVR generated stable cell lines, conducted the statistical analyses, participated in xenograft experiments, drafting, revising and editing of the manuscript, as well as participated in the concept and design of the studies. HCS performed the qPCR arrays and participated in critical revision of the manuscript. JLD was involved in the xenograft experiments and manuscript revision. FNP conducted the antigen retrieval, staining and visualization of the primary tumor tissues as well as manuscript revision. MEB participated in the concept and design of the study and revising and editing of the manuscript. BMC conceived of the study, participated in the study design and revising and editing of the manuscript. All authors have read and approved of the final manuscript.

Acknowledgements

The authors would like to acknowledge Dr. Kenneth Nephew and Dr. Brian Rowan for critical review of this manuscript. We also acknowledge the expert skills and advice of Mary Price and the Louisiana Cancer Research Consortium FACS Core Facility. This research was supported by: Susan G. Komen Breast Cancer Foundation BCTR0601198 (ME Burow); The Department of Defense Breast Cancer Research Program BC085426 (BM Collins-Burow); The National Institutes of Health/National Center for Research Resources P20RR020152 (BM Collins-Burow) and CA125806 (ME Burow). The funders did not have any involvement in study design; the collection, analysis, or interpretation of the data; the writing of the manuscript; or the decision to submit the manuscript for publication.

References

1. Jemal A, Bray F, Center MM, Ferlay J, Ward E, Forman D: **Global cancer statistics**. *CA: A Cancer Journal for Clinicians* 2011, **61**(2):69-90.
2. Fernandez Y, Cueva J, Palomo AG, Ramos M, de Juan A, Calvo L, Garcia-Mata J, Garcia-Teijido P, Pelaez I, Garcia-Estevez L: **Novel therapeutic approaches to the treatment of metastatic breast cancer**. *Cancer Treat Rev* 2010, **36**(1):33-42.
3. Beaumont T, Leadbeater M: **Treatment and care of patients with metastatic breast cancer**. *Nurs Stand* 2011, **25**(40):49-56.
4. Schneider BP, Winer EP, Foulkes WD, Garber J, Perou CM, Richardson A, Sledge GW, Carey LA: **Triple-negative breast cancer: risk factors to potential targets**. *Clin Cancer Res* 2008, **14**(24):8010-8018.
5. Dent R, Trudeau M, Pritchard KI, Hanna WM, Kahn HK, Sawka CA, Lickley LA, Rawlinson E, Sun P, Narod SA: **Triple-Negative Breast Cancer: Clinical Features and Patterns of Recurrence**. *Clinical Cancer Research* 2007, **13**(15):4429-4434.
6. Elias AD: **Triple-negative breast cancer: a short review**. *Am J Clin Oncol* 2010, **33**(6):637-645.
7. Anders CK, Carey LA: **Biology, metastatic patterns, and treatment of patients with triple-negative breast cancer**. *Clin Breast Cancer* 2009, **9 Suppl 2**:S73-81.
8. Hudis CA, Gianni L: **Triple-negative breast cancer: an unmet medical need**. *Oncologist* 2011, **16 Suppl 1**:1-11.
9. De Laurentiis M, Cianniello D, Caputo R, Stanzione B, Arpino G, Cinieri S, Lorusso V, De Placido S: **Treatment of triple negative breast cancer (TNBC): current options and future perspectives**. *Cancer Treat Rev* 2010, **36 Suppl 3**:S80-86.

10. Chacon RD, Costanzo MV: **Triple-negative breast cancer**. *Breast Cancer Res* 2010, **12 Suppl 2**:S3.

11. Drummond DC, Noble CO, Kirpotin DB, Guo Z, Scott GK, Benz CC: **Clinical development of histone deacetylase inhibitors as anticancer agents**. *Annu Rev Pharmacol Toxicol* 2005, **45**:495-528.

12. Liu T, Kuljaca S, Tee A, Marshall GM: **Histone deacetylase inhibitors: multifunctional anticancer agents**. *Cancer Treat Rev* 2006, **32**(3):157-165.

13. Vigushin DM, Coombes RC: **Histone deacetylase inhibitors in cancer treatment**. *Anticancer Drugs* 2002, **13**(1):1-13.

14. Lin HY, Chen CS, Lin SP, Weng JR, Chen CS: **Targeting histone deacetylase in cancer therapy**. *Med Res Rev* 2006, **26**(4):397-413.

15. Kikuchi H, Barman HK, Nakayama M, Takami Y, Nakayama T: **Participation of histones, histone modifying enzymes and histone chaperones in vertebrate cell functions**. *Subcell Biochem* 2006, **40**:225-243.

16. Konstantinopoulos PA, Karamouzis MV, Papavassiliou AG: **Focus on acetylation: the role of histone deacetylase inhibitors in cancer therapy and beyond**. *Expert Opin Investig Drugs* 2007, **16**(5):569-571.

17. Xu WS, Parmigiani RB, Marks PA: **Histone deacetylase inhibitors: molecular mechanisms of action**. *Oncogene* 2007, **26**(37):5541-5552.

18. Atadja P: **Development of the pan-DAC inhibitor panobinostat (LBH589): successes and challenges**. *Cancer Lett* 2009, **280**(2):233-241.

19. Dokmanovic M, Clarke C, Marks PA: **Histone deacetylase inhibitors: overview and perspectives**. *Mol Cancer Res* 2007, **5**(10):981-989.

20. Shao W, Growney JD, Feng Y, O'Connor G, Pu M, Zhu W, Yao YM, Kwon P, Fawell S, Atadja P: **Activity of deacetylase inhibitor panobinostat (LBH589) in cutaneous T-cell lymphoma models: Defining molecular mechanisms of resistance**. *Int J Cancer* 2010, **127**(9):2199-2208.

21. Maiso P, Carvajal-Vergara X, Ocio EM, Lopez-Perez R, Mateo G, Gutierrez N, Atadja P, Pandiella A, San Miguel JF: **The histone deacetylase inhibitor LBH589 is a potent antimyeloma agent that overcomes drug resistance**. *Cancer Res* 2006, **66**(11):5781-5789.

22. Giles F, Fischer T, Cortes J, Garcia-Manero G, Beck J, Ravandi F, Masson E, Rae P, Laird G, Sharma S *et al*: **A phase I study of intravenous LBH589, a novel cinnamic hydroxamic acid analogue histone deacetylase inhibitor, in patients with refractory hematologic malignancies**. *Clin Cancer Res* 2006, **12**(15):4628-4635.

23. Fukutomi A, Hatake K, Matsui K, Sakajiri S, Hirashima T, Tanii H, Kobayashi K, Yamamoto N: **A phase I study of oral panobinostat (LBH589) in Japanese patients with advanced solid tumors**. *Invest New Drugs* 2011.

24. Catalano MG, Pugliese M, Gargantini E, Grange C, Bussolati B, Asioli S, Bosco O, Poli R, Compagnone A, Bandino A *et al*: **Cytotoxic activity of the histone deacetylase inhibitor panobinostat (LBH589) in anaplastic thyroid cancer in vitro and in vivo**. *International Journal of Cancer* 2012:n/a-n/a.

25. Crisanti MC, Wallace AF, Kapoor V, Vandermeers F, Dowling ML, Pereira LP, Coleman K, Campling BG, Fridlender ZG, Kao GD *et al*: **The HDAC inhibitor panobinostat (LBH589) inhibits mesothelioma and lung cancer cells in vitro and in vivo with particular efficacy for small cell lung cancer**. *Mol Cancer Ther* 2009, **8**(8):2221-2231.

26. Prince HM, Bishton MJ, Johnstone RW: **Panobinostat (LBH589): a potent pan-deacetylase inhibitor with promising activity against hematologic and solid tumors**. *Future Oncol* 2009, **5**(5):601-612.

27. Geng L, Cuneo KC, Fu A, Tu T, Atadja PW, Hallahan DE: **Histone deacetylase (HDAC) inhibitor LBH589 increases duration of gamma-H2AX foci and confines HDAC4 to the cytoplasm in irradiated non-small cell lung cancer**. *Cancer Res* 2006, **66**(23):11298-11304.

28. Catley L, Weisberg E, Kiziltepe T, Tai YT, Hideshima T, Neri P, Tassone P, Atadja P, Chauhan D, Munshi NC *et al*: **Aggresome induction by proteasome inhibitor bortezomib and alpha-tubulin hyperacetylation by tubulin deacetylase (TDAC) inhibitor LBH589 are synergistic in myeloma cells**. *Blood* 2006, **108**(10):3441-3449.

29. Maiso P, Colado E, Ocio EM, Garayoa M, Martin J, Atadja P, Pandiella A, San-Miguel JF: **The synergy of panobinostat plus doxorubicin in acute myeloid leukemia suggests a role for HDAC inhibitors in the control of DNA repair**. *Leukemia* 2009, **23**(12):2265-2274.

30. Rathkopf D, Wong BY, Ross RW, Anand A, Tanaka E, Woo MM, Hu J, Dzik-Jurasz A, Yang W, Scher HI: **A phase I study of oral panobinostat alone and in combination with docetaxel in patients with castration-resistant prostate cancer**. *Cancer Chemother Pharmacol* 2010, **66**(1):181-189.

31. Ellis L, Pan Y, Smyth GK, George DJ, McCormack C, Williams-Truax R, Mita M, Beck J, Burris H, Ryan G *et al*: **Histone deacetylase inhibitor panobinostat induces clinical responses with associated alterations in gene expression profiles in cutaneous T-cell lymphoma**. *Clin Cancer Res* 2008, **14**(14):4500-4510.

32. Drappatz J, Lee EQ, Hammond S, Grimm SA, Norden AD, Beroukhim R, Gerard M, Schiff D, Chi AS, Batchelor TT *et al*: **Phase I study of panobinostat in combination with bevacizumab for recurrent high-grade glioma**. *J Neurooncol* 2011.

33. Lemoine M, Younes A: **Histone deacetylase inhibitors in the treatment of lymphoma**. *Discov Med* 2010, **10**(54):462-470.

34. Rhodes LV, Muir SE, Elliott S, Guillot LM, Antoon JW, Penfornis P, Tilghman SL, Salvo VA, Fonseca JP, Lacey MR *et al*: **Adult human mesenchymal stem cells enhance breast tumorigenesis and promote hormone independence**. *Breast Cancer Res Treat* 2010, **121**(2):293-300.

35. Semb H, Christofori G: **The tumor-suppressor function of E-cadherin**. *Am J Hum Genet* 1998, **63**(6):1588-1593.

36. Hugo H, Ackland ML, Blick T, Lawrence MG, Clements JA, Williams ED, Thompson EW: **Epithelial—mesenchymal and mesenchymal—epithelial transitions in carcinoma progression**. *Journal of Cellular Physiology* 2007, **213**(2):374-383.

37. Blick T, Widodo E, Hugo H, Waltham M, Lenburg ME, Neve RM, Thompson EW: **Epithelial mesenchymal transition traits in human breast cancer cell lines**. *Clin Exp Metastasis* 2008, **25**(6):629-642.

38. Pishvaian MJ, Feltes CM, Thompson P, Bussemakers MJ, Schalken JA, Byers SW: **Cadherin-11 is expressed in invasive breast cancer cell lines**. *Cancer Res* 1999, **59**(4):947-952.

39. Kalin JH, Butler KV, Kozikowski AP: **Creating zinc monkey wrenches in the treatment of epigenetic disorders**. *Current Opinion in Chemical Biology* 2009, **13**(3):263-271.

40. Terpos E: **The synergistic effect of panobinostat (LBH589) with melphalan or doxorubicin on multiple myeloma cells; rationale for the use of combination regimens in myeloma patients**. *Leuk Res* 2010, **35**(3):295-296.

41. Nishioka C, Ikezoe T, Yang J, Komatsu N, Bandobashi K, Taniguchi A, Kuwayama Y, Togitani K, Koeffler HP, Taguchi H: **Histon deacetylase inhibitors induce growth arrest and apoptosis of HTLV-1-infected T-cells via blockade of signaling by nuclear factor kappaB**. *Leuk Res* 2008, **32**(2):287-96.

42. Di Fazio P, Schneider-Stock R, Neureiter D, Okamoto K, Wissniowski T, Gahr S, Quint K, Meissnitzer M, Alinger B, Montalbano R *et al*: **The pan-deacetylase inhibitor panobinostat inhibits growth of hepatocellular carcinoma models by alternative pathways of apoptosis**. *Cell Oncol* 2010, **32**(4):285-300.

43. Zhou Q, Atadja P, Davidson NE: **Histone deacetylase inhibitor LBH589 reactivates silenced estrogen receptor alpha (ER) gene expression without loss of DNA hypermethylation**. *Cancer Biol Ther* 2007, **6**(1):64-69.

44. Fortunati N, Catalano MG, Marano F, Mugoni V, Pugliese M, Bosco O, Mainini F, Boccuzzi G: **The pan-DAC inhibitor LBH589 is a multi-functional agent in breast cancer cells: cytotoxic drug and inducer of sodium-iodide symporter (NIS)**. *Breast Cancer Res Treat* 2010, **124**(3):667-675.

45. Budman DR, Tai J, Calabro A, JohnV: **The histone deacetylase inhibitor panobinostat demonstrates marked synergy with conventional chemotherapeutic agents in human ovarian cancer cell lines**. *Invest New Drugs* 2011, **29**(6):1224-9.

46. Storch K, Eke I, Borgmann K, Krause M, Richter C, Becker K, Schröck E, Cordes N: **Three-dimensional cell growth confers radioresistance by chromatin density modification**. *Cancer Res* 2010, **70**(10):3925-34.

47. Rao R, Balusu R, Fiskus W, Mudunuru U, Venkannagari S, Chauhan L, Smith JE, Hembruff SL, Ha K, Atadja PW, Bhalla KN: **Combination of pan-histone deacetylase inhibitor and autophagy inhibitor exerts superior efficacy against triple-negative human breast cancer cells**. *Mol Cancer Ther* 2012, Epub ahead of print.

48. Thomas S, Thurn KT, Biçaku E, Marchion DC, Münster PN: **Addition of a histone deacetylase inhibitor redirects tamoxifen-treated breast cancer cells into apoptosis, which is opposed by induction of autophagy**. *Breast Cancer Res Treat* 2011, **130**(2):437-47.

49. Chen S, Ye J, Kijima I, Evans D: **The HDAC inhibitor LBH589 (panobinostat) is an inhibitory modulator of aromatase gene expression**. *Proc Natl Acad Sci USA* 2010, **107**(24):11032-7.

50. Palmieri D, Lockman PR, Thomas FC, Hua E, Herring J, Hargrave E, Johnson M, Flores N, Qian Y, Vega-Valle E *et al*: **Vorinostat inhibits brain metastatic colonization in a model of triple-negative breast cancer and induces DNA double-strand breaks**. *Clin Cancer Res* 2009, **15**(19):6148-6157.

51. Floris G, Debiec-Rychter M, Sciot R, Stefan C, Fieuws S, Machiels K, Atadja P, Wozniak A, Faa G, Schoffski P: **High Efficacy of Panobinostat Towards Human Gastrointestinal Stromal Tumors in a Xenograft Mouse Model**. *Clinical Cancer Research* 2009, **15**(12):4066-4076.

52. Neve RM, Chin K, Fridlyand J, Yeh J, Baehner FL, Fevr T, Clark L, Bayani N, Coppe JP, Tong F *et al*: **A collection of breast cancer cell lines for the study of functionally distinct cancer subtypes**. *Cancer Cell* 2006, **10**(6):515-527.

53. Prat A, Parker JS, Karginova O, Fan C, Livasy C, Herschkowitz JI, He X, Perou CM: **Phenotypic and molecular characterization of the claudin-low intrinsic subtype of breast cancer**. *Breast Cancer Res* 2010, **12**(5):R68.

54. Zajchowski DA, Bartholdi MF, Gong Y, Webster L, Liu HL, Munishkin A, Beauheim C, Harvey S, Ethier SP, Johnson PH: **Identification of gene expression profiles that predict the aggressive behavior of breast cancer cells**. *Cancer Res* 2001, **61**(13):5168-5178.

55. Sommers CL, Byers SW, Thompson EW, Torri JA, Gelmann EP: **Differentiation state and invasiveness of human breast cancer cell lines**. *Breast Cancer Res Treat* 1994, **31**(2-3):325-335.

56. Kenny PA, Lee GY, Myers CA, Neve RM, Semeiks JR, Spellman PT, Lorenz K, Lee EH, Barcellos-Hoff MH, Petersen OW *et al*: **The morphologies of breast cancer cell lines in three-dimensional assays correlate with their profiles of gene expression**. *Mol Oncol* 2007, **1**(1):84-96.

57. Drasin DJ, Robin TP, Ford HL: **Breast cancer epithelial-to-mesenchymal transition: examining the functional consequences of plasticity**. *Breast Cancer Res* 2011, **13**(6):226.

58. Ouyang G: **Epithelial-Mesenchymal Transition and Cancer Stem Cells**. In: *Cancer Stem Cells - The Cutting Edge Stanley Shostak (Ed).* vol. August 2011: InTech; 2011.

59. Kalluri R, Weinberg RA: **The basics of epithelial-mesenchymal transition**. *J Clin Invest* 2009, **119**(6):1420-1428.

60. May CD, Sphyris N, Evans KW, Werden SJ, Guo W, Mani SA: **Epithelial-mesenchymal transition and cancer stem cells: a dangerously dynamic duo in breast cancer progression**. *Breast Cancer Res* 2011, **13**(1):202.

61. Morrogh M, Andrade VP, Giri D, Sakr RA, Paik W, Qin LX, Arroyo CD, Brogi E, Morrow M, King TA: **Cadherin-catenin complex dissociation in lobular neoplasia of the breast**. *Breast Cancer Res Treat* 2011.

62. Kuniyasu H, Ellis LM, Evans DB, Abbruzzese JL, Fenoglio CJ, Bucana CD, Cleary KR, Tahara E, Fidler IJ: **Relative expression of E-cadherin and type IV collagenase genes predicts disease outcome in patients with resectable pancreatic carcinoma**. *Clin Cancer Res* 1999, **5**(1): 25-33.

Figure Legends

Figure 1. LBH589 increases histone H3 (Lys9) and H4 (Lys8) acetylation in TNBC cell lines. Cells were treated with LBH589 (100, 200nM) or vehicle (DMSO) for 18 hours, fixed, permeabilized and stained for acetyl-histones **(A)** H3 (Lys9) or **(B)** H4 (Lys8) and subjected to flow cytometry**.** Data is presented as mean fluorescence intensity (mean ± SEM) of two independent experiments, (***, $p<0.001$). **(C-D)** Confocal images of TNBC cell lines treated with LBH589 (100nM) or vehicle for 18 hours, fixed, permeabilized and stained red [Rhodamine Phalloidin] for actin filaments and green [Alexa Fluor® 488] for acetyl-histones **(C)** H3 (Lys9) or **(D)** H4 (Lys8). Original magnification was 400x with scale bars at 20 microns.

Figure 2. LBH589 decreases TNBC cell proliferation and viability. Cells from four TNBC cell lines (MDA-MB-157, MDA-MB-231, MDA-MB-468, BT549) and three ER-positive cell lines (MCF-7, MDA-MB-361, ZR-75) were treated with LBH589 (50, 100, 200 nM) or vehicle (DMSO) for 24 hours and assayed by **(A)** MTT proliferation and **(B)** trypan blue exclusion assays**.** Data is represented as percent control (mean ± SEM) of three independent experiments, (**, $p<0.01$; ***, $p<0.001$).

Figure 3. LBH589 induces apoptosis in TNBC cells. **(A)** TNBC cells treated with LBH589 (100, 200nM) or vehicle (DMSO) for 24 hours were assayed by DNA fragmentation (Cell Death ELISA) assay to assess changes in apoptosis**.** Data is presented as enrichment (mean ± SEM) versus control of two independent experiments (***, $p<0.001$). **(B)** Representative confocal images show presence of apoptotic bodies (arrows) in LBH589 treated MDA-MB-157, MDA-MB-231, and BT-549 cells at 18 hours. Cells stained red [rhodamine phalloidin] for actin

filaments, green [Alexa Fluor® 488] for acetyl-histone H3 (Lys9), and blue for DAPI nuclear stain. Original magnification is 400x with scale bars at 20 microns.

Figure 4. Effect of LBH589 on tumor growth in MDA-MB-231 and BT549 xenograft models. Female, CB-17/SCID mice (n=5/group) were injected with **(A)** MDA-MB-231-tRFP or **(B)** BT-549-tRFP cells ($5x10^6$ cells/injection) bilaterally into the inguinal mammary fat pad. On day 14, mice were treated intraperitoneally (i.p.) with LBH589 (10mg/kg) or vehicle (1:20 DMSO in normal saline) 5 days/week for 28 days. Data points represent average tumor volume ± SEM, (***, $p<0.001$).

Figure 5. Heat Map of LBH589-induced gene expression changes in MDA-MB-231, MDA-MB-468, and MCF-7 cells. MDA-MB-231, MDA-MB-468, or MCF-7 cells were treated for 24 hours with LBH589 (100nM) or vehicle (DMSO) and then assayed via the Human Breast Cancer and Estrogen Receptor Signaling RT² Profiler™ PCR Array. Red signifies up-regulation and green signifies down-regulation by LBH589 compared to MDA-MB-231 vehicle treated controls. Data is representative of three independent experiments. Genes regulated at least 2-fold are also summarized in **Supplemental Tables 1** (MDA-MB-231), **2** (MDA-MB-468) **and 3** (MCF-7).

Figure 6. LBH589 up-regulates CDH1 expression and initiates EMT reversal in MDA-MB-231 Cells. MDA-MB-231 cells were plated overnight and treated with LBH589 (100nM) or vehicle (DMSO) for 24 hours. The expression of CDH1 was examined by **(A)** flow cytometry and **(B)** ELISA. Data is represented as mean ± SEM of two independent experiments, (***, $p<0.001$). **(C-E)** MDA-MB-231 morphology changes were assessed in vehicle and LBH589 (100nM) treated cells with 3-color fluorescence staining on a BD Pathway 855 Bioimager. **(C)**

Control and **(D-E)** LBH589 treated cells were stained red [rhodamine phalloidin] for actin filaments, green [Alexa Fluor® 488] for acetyl-histone H3 (Lys9), and blue [DAPI] nuclear counter stain. Partial reversal of EMT in treated cells is indicated by presence of cuboidal/spherical cells (arrows). **(E)** 2-fold magnification of field with normal untransformed mesenchymal cell and transformed spherical cells. Original magnification is 400x with scale bars at 20 microns.

Figure 7. LBH589 increases CDH1 expression in MDA-MB-231 primary tumors.

Control and LBH589 treated, formalin-fixed mammary fat pad sections from MDA-MB-231-tRFP injected CB17-SCID mice were stained for hematoxylin and eosin (left column) or anti-human CDH1 (1:30; right column) followed by Alexa Fluor® 488 secondary antibody. Original magnification was 100x with scale bars at 200 microns.

Additional Files:

Supplemental Table 1 - LBH589 induced expression changes of breast cancer related genes in MDA-MB-231 cells.

Supplemental Table 2 - LBH589 induced expression changes of breast cancer related genes in MDA-MB-468 cells.

Supplemental Table 3 - LBH589 induced expression changes of breast cancer related genes in MCF-7 cells.

Table1. Effect 100nM LBH589 on Cell cycle percentage of TNBC cells.

	LBH589		G0/G1	S	G2/M
MDA-MB-157	-	24h	61.72	21.68	16.59
	+	24h	64.3	10.83	24.87
	-	72h	52.21	25.53	22.26
	+	72h	54.14	9.48	36.37
MDA-MB-231	-	24h	86.74	6.03	7.23
	+	24h	33.04	0.5	66.46
	-	72h	57.05	24.7	18.25
	+	72h	37.75	2.33	59.92
MDA-MB-468	-	24h	54.07	30.29	15.64
	+	24h	51.55	17.01	31.44
	-	72h	53.45	34.81	11.74
	+	72h	52.67	16.78	30.55
BT-549	-	24h	37.66	26.57	35.77
	+	24h	39.76	8.61	51.63
	-	72h	36.42	27.08	36.49
	+	72h	42.93	3.95	53.13

Data (percent gated cells) representative of two independent experiments.

Supplemental Table 1. LBH589 induced expression changes of breast cancer related genes in MDA-MB-231 cells.

Gene	Fold Change	p-value	Gene	Fold Change	p-value
C3	14.2811	0.000787	JUN	2.0972	0.018841
CCNA1	2.1187	0.000251	KRT19	3.0201	0.004639
CCNA2	-7.9516	0.000263	MKI67	-5.3952	0.003995
CCND1	-2.3645	0.008124	MT3	87.5637	0.000006
CDH1	31.5314	0.000109	NGFR	5.9384	0.001183
CLDN7	2.8327	0.036800	**PLAU**	-3.6183	0.004041
CLU	4.833	0.021822	PTGS2	3.9591	0.000003
DLC1	2.4499	0.018090	SCGB2A1	2.8009	0.012118
ESR2	3.1422	0.038547	SERPINB5	16.6616	0.000233
FAS	-2.5629	0.000034	SERPINE1	3.6917	0.008257
FASLG	9.1408	0.010602	**STC2**	5.3278	0.001767
FOSL1	-2.7357	0.000378	TFF1	3.6224	0.003828
GATA3	-2.6459	0.012088	**TGFA**	-2.0492	0.008134
GSN	3.2493	0.000240	**THBS2**	13.9506	0.000027
ID2	15.6074	0.001580	**TNFAIP2**	-3.0531	0.037264
IGFBP2	12.9484	0.021366	TOP2A	-3.5808	0.010860
IL6	2.7785	0.000187	TP53	-5.7928	0.004610
IL6R	4.7075	0.002408			

Data (expressed as fold change vs. controls) representative of three independent experiments ($p<0.05$). Up-regulated genes are in red, down-regulated genes are in blue.

Supplemental Table 2. LBH589 induced expression changes of breast cancer related genes in MDA-MB-468 cells.

Gene	Fold Change	p-value	Gene	Fold Change	p-value
CCNA1	25.69	0.004405	MT3	2.58	0.047406
CCNA2	-2.89	0.000510	MUC1	-3.26	0.004271
CCNE1	2.06	0.034962	NGFR	8.25	0.001621
CDKN1A	4.57	0.001671	PAPPA	3.46	0.002328
COL6A1	9.08	0.000665	RAC2	2.28	0.023474
CYP19A1	10.69	0.001384	SCGB1D2	-10.05	0.000329
FOSL1	3.88	0.009441	SERPINB5	3.29	0.011926
IGFBP2	3.87	0.005641	SERPINE1	9.40	0.004054
IL6	36.21	0.000351	SPRR1B	10.61	0.000177
IL6R	4.32	0.012499	TFF1	7.29	0.002060
ITGB4	3.15	0.001689	THBS1	2.08	0.001811
MKI67	-2.66	0.005104	TOP2A	-2.85	0.047559

Data (expressed as fold change vs. controls) representative of three independent experiments ($p<0.05$). Up-regulated genes are in red, down-regulated genes are in blue.

Supplemental Table 3. LBH589 induced expression changes of breast cancer related genes in MCF-7 cells.

Gene	Fold Change	p-value	Gene	Fold Change	p-value
C3	221.67	0.036263	JUN	3.90	0.028618
CCNA1	133.37	0.011505	KLF5	2.93	0.043037
CCNA2	-11.71	0.000044	KLK5	6.48	0.015973
CCND1	-5.47	0.041624	KRT19	2.22	0.027859
CDKN1A	7.16	0.000022	MKI67	-8.09	0.001231
CLU	8.79	0.000165	MT3	13.03	0.035126
COL6A1	2.91	0.002925	NGFR	87.64	0.012465
DLC1	2.46	0.021622	NME1	-2.19	0.006751
ESR1	-4.13	0.000053	PGR	-2.02	0.035412
ESR2	3.18	0.038440	PTGS2	4.76	0.024590
FGF1	2.63	0.013574	SCGB1D2	7.01	0.019844
GSN	3.40	0.000614	SCGB2A1	106.52	0.005723
HMGB1	-4.49	0.003741	SERPINB5	32.51	0.005101
ID2	4.90	0.005877	SERPINE1	43.76	0.001627
IL6	26.13	0.000382	SLC7A5	2.70	0.005534
IL6R	-2.44	0.012947	TOP2A	-2.75	0.008773
ITGA6	4.07	0.006897	TP53	-12.06	0.006725

Data (expressed as fold change vs. controls) representative of three independent experiments ($p<0.05$). Up-regulated genes are in red, down-regulated genes are in blue.